Ceramic tooth root implants in dogs:

Design and clinical evaluation

by

Gabriele Gruss Niederauer

A Thesis Submitted to the

Graduate Faculty in Partial Fulfillment of the

Requirements for the Degree of

MASTER OF SCIENCE

Departments: Materials Science and Engineering
             Biomedical Engineering
Co-Majors: Ceramic Engineering
            Biomedical Engineering

Iowa State University
Ames, Iowa

1990

TABLE OF CONTENTS

LIST OF TABLES

LIST OF FIGURES

INTRODUCTION

In cases where the natural teeth are missing, dental implants can be an alternative to dentures and bridges by providing permanent tooth structures. In 1984, a study estimated that there are 20 million edentulous persons in the United States, of which at least 20 % were dissatisfied with their dentures (Stanley et al., 1986). Dental tooth root implants pose a challenging problem because of their transcutaneous nature and exposure to the hostile oral environment.

Various materials, such as metals, ceramics and polymers, have been studied. For tooth root implant purposes, ceramics offer many advantages over other biomaterials because of their biocompatibility and corrosion resistance. One particular ceramic biomaterial, named osteoceramic, is being studied as a tooth root implant material. It is composed of $\alpha\text{-Ca}_3(PO_4)_2$ and $MgAl_2O_4$ spinel. This ceramic composite is biologically active due to the calcium phosphate phase and strong because of the strength and the low solubility of the inert spinel. In a previous study, subgingival tooth root implants made of the osteoceramic were found to have good bone response (Tweden, 1987). However, in order to make a tooth root functional, it must protrude through the gingiva

to support a crown or bridge. Consequently, it would be desirable for the permucosal interface between the implant and gingiva to form a seal to keep oral bacteria from penetrating. The physical and chemical properties of other implants in contact with the gingiva have been found to affect this attachment mechanism (Salthouse and Matlaga, 1983).

The goals of this study were to design, implant and clinically evaluate the osteoceramic tooth root placed in the canine mandible. The objective of this research was to test two hypotheses: (1) that the soft tissue structure can be influenced by varying the implant surface properties, and (2) that there is an optimum shoulder height for an implant that is initially covered and then exposed.

Forty tooth root implants were manufactured with equal molar quantities of magnesium aluminate spinel and α-calcium phosphate tribasic. After firing the implants to 1450°C, the shoulder bands were etched, polished, or left as fired to produce rough, smooth, and irregular surfaces, respectively. The different surfaces were characterized to determine pore structure. The design of the implant will allow these surfaces to be directly adjacent to the gingiva. Thirty-two implants with varying shoulder heights

and/or varying surface structures were placed in eight mongrel dogs. These implants remained covered during the initial healing period after which the gingiva was cut back to expose the implants. Eight subgingival implants were placed in two dogs for shorter time periods to study the healing process at 20 and 33 days. Radiographic and clinical examinations were performed to evaluate tissue response by measuring gingival bleeding, mobility, plaque and calculus, sulcus depth, radiographic bone response and vertical alveolar bone ridge loss.

LITERATURE REVIEW

The literature review is composed of four major sections: dental anatomy, implant design, current status of dental implants and calcium phosphates as dental implants. The first section, dental anatomy, gives the reader some background about the structure and function of natural teeth, the gingival epithelium and the connective tissues of the periodontium. The second section, implant design, discusses the materials, the shapes and surface topographies which have been used for implants and the responses which have been found. The third section, current status of dental implants, gives the present use of dental implants in clinical and research applications. The last section, calcium phosphates as biomaterials, focuses on hydroxyapatite, tricalcium phosphates, and a calcium phosphate/magnesium aluminate spinel composite for use as a dental implant material.

Dental Anatomy

The jaw has two bones: the maxilla, the upper jaw, and the mandible, the lower jaw. These two bones act as the foundation for the soft tissues of the oral cavity and the face (Ranly, 1976). The main components of the jaws include the alveolar bone, the gingival epithelium and the teeth.

Teeth

Natural teeth are positioned in the alveolar sockets
in the jaw. The alveolar bone is covered by gingiva,
whereas the alveolar sockets are lined with the periodontal
membrane or ligament. As shown in Figure 1, the tooth has
three portions: the crown, the neck and the root. The
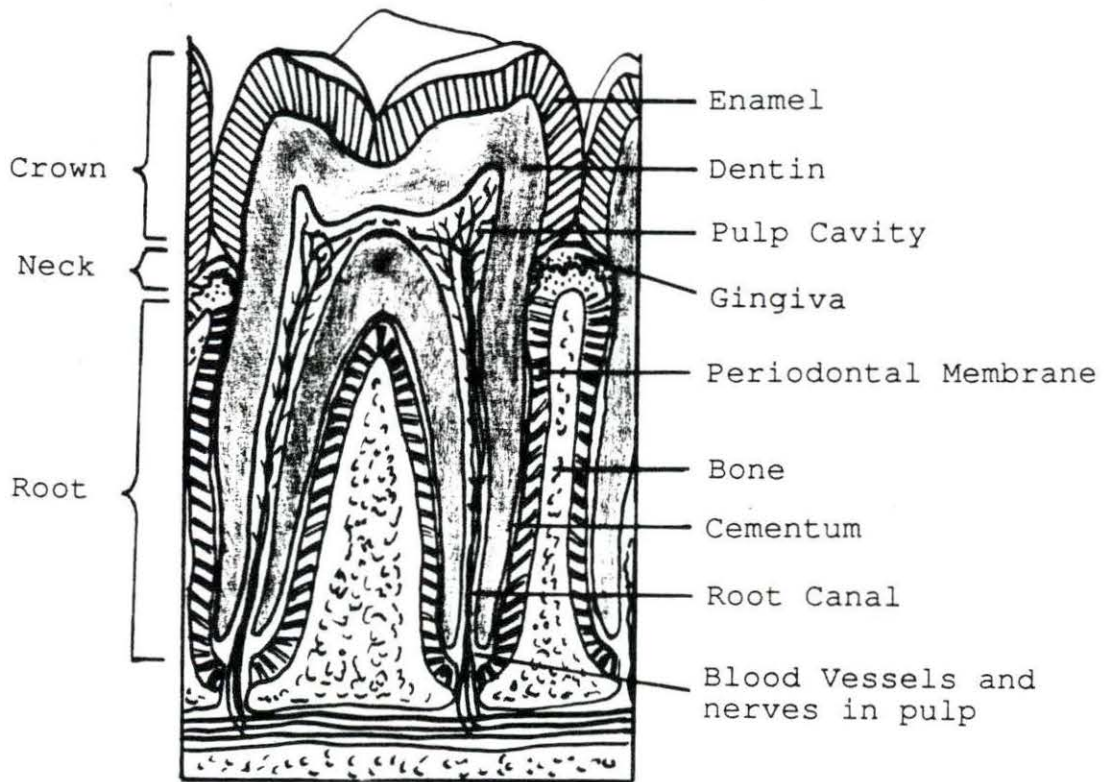
Figure 1.   Longitudinal section of a molar tooth within an
             alveolus (Spence and Mason, 1987)

crown extends above the gingiva and has enamel as its outer
layer. The neck is the slightly constricted area of the
tooth, between the crown and the root, to which the gingiva
is attached (Spence and Mason, 1987). The root is
submerged below the gingiva and anchors the tooth in place.
The blood vessels and nerves to the pulp cavity run through
the root canal to supply nutrition and innervation to the
tooth.

The tooth does not have one single composition since
age, diet, position in the mouth, health condition and
medical history all affect it (Lazzari, 1976). Lefevre and
Hodge (1937) found teeth to have the inorganic components
listed in Table 1.

Table 1. Inorganic chemical composition of human teeth
          (Lefevre and Hodge, 1937)

Mineral Content	Weight (%)
water	8.98
calcium	35.20
phosphorus	16.80
magnesium	0.32
carbonate	3.45

From these data, the calcium/phosphorus ratio of the tooth
calculates to be 2.1. The components for enamel and dentin
vary slightly from those given in Table 1 for teeth.

The tooth is subjected to the hostile environment of
the oral cavity, which is continually changing its chemical
composition, pH, bacterial flora and temperature. In
addition, teeth are exposed to the masticatory forces.
Colaizzi et al. (1984) found that during normal human
dentition, the tooth is subjected to an axial force in the
range of 200-2440 N. In addition, Graf (1969) found the
lateral component of the biting force in adults to be
approximately 20 N.

Gingival epithelium

The factors which affect the structure and metabolism
of gingival epithelium are age, hormones and nutrition.
Like other epithelia, gingival epithelium is supported by
connective tissue from which the cells obtain their
metabolic requirements and through which the products of
metabolism are dispersed (Smith, 1969). The function of
the epithelium in the gingival region is mainly protection.
The gingival epithelium is multilayered, capable of
continuous renewal, and covered in part by a surface layer
of keratin. Figure 2 shows the alveolar mucosa and the
three components of the gingival epithelium: the alveolar

Marginal Gingiva

Connective Tissue

Attached Gingiva

Periodontal
Membrane

Cementum

Alveolar Mucosa

Alveolar Bone

Gingival Crevice

Crevicular Epithelium

Attached Epithelial
Cuff

Masticatory
Epithelium

Keratin

Mucogingival
Line

Basement Membrane
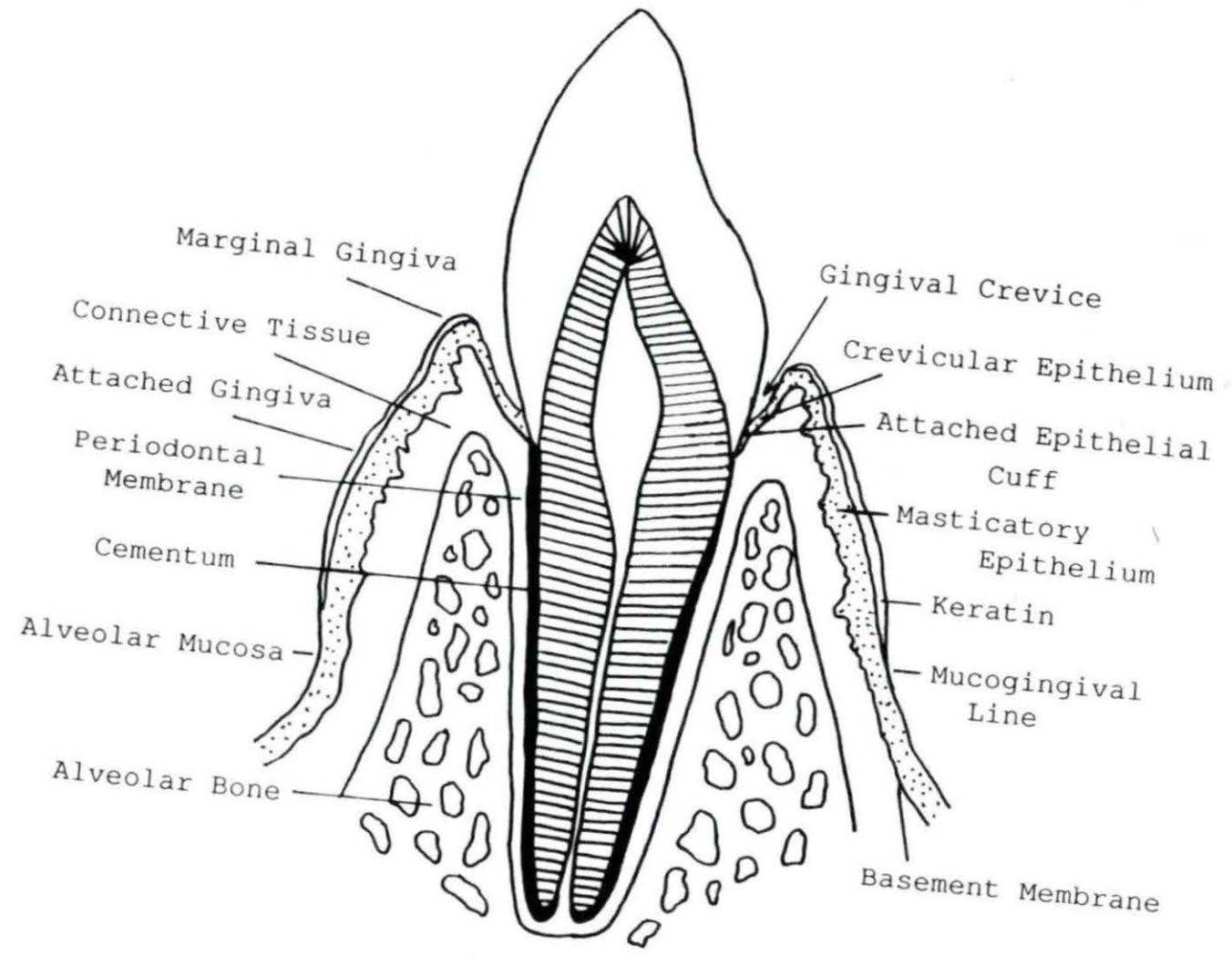
Figure 2.   Vertical section through a tooth and its supporting structures (Smith, 1969)

mucosa, the masticatory epithelium, the crevicular epithelium and the attached epithelial cuff.

Alveolar mucosa   The mucogingival line divides the masticatory gingival epithelium and the alveolar mucosa. The microscopic differences between these two is that the masticatory gingiva is keratinized and has no elastic fibers present, whereas the alveolar mucosa is not keratinized but has elastic fibers present in its connective tissue (Smith, 1969) The function of each tissue causes this difference in structure. The keratinized surfaces of the masticatory gingiva provide protection against abrasive forces, whereas the elastic fibers of the alveolar mucosa give it elastic flexibility.

Masticatory epithelium   The masticatory gingival epithelium includes the attached, marginal and crestal gingival epithelium (Smith, 1969). The attached gingiva is the gingival mucosa from the mucogingival line to the gingival margin. Its name comes from it being firmly bound to the underlying alveolar bone and partially to the cementum. The marginal gingiva lies adjacent to the coronal region, and the crestal gingiva is the area at the apex of the gingival epithelium. Neither of these is attached to the alveolar bone or cementum.

The masticatory gingival epithelium is stratified squamous and is supported by a dense fibrous corium. The two layers are separated from each other by a thin basement membrane. This membrane has deep and irregular, wave-like elevated papillae on the surface of the connective tissue to protect it from shearing stresses (Smith, 1969). Invaginations between the papillae are occupied by downgrowths of epithelium called rete ridges (Smith, 1969). The epithelium has an average depth of 12-13 cells (Gargiulo et al., 1961). Keratin flakes are discarded from the surface during normal wear and tear and are then replaced by differentiation from deeper layers (Smith, 1969).

Crevicular epithelium   The crevicular gingival epithelium spans from the gingival margin to the most coronal point of the attached epithelial cuff. It consists of a thin layer of stratified squamous epithelial cells which is 5-15 cells in depth (Smith, 1969). This epithelium forms a soft tissue lining of the shallow gingival crevice encircling each tooth and becomes thinner as the cuff is approached. It is supported by dense fibrous connective tissue and is not related to the alveolar bone. Compared to the masticatory epithelium, the crevicular gingival epithelium is thinner, is not

keratinized and has no rete ridges (Smith, 1969). The
basement membrane of the crevicular gingival epithelium
appears smooth and regular. Desquamation, shedding of the
cuticle in scales, occurs which implies that dividing cells
are present somewhere in the epithelium (Smith, 1969).

    <u>Attached epithelial cuff</u>   The attached epithelial
cuff is the attachment mechanism between the gingival
epithelium and the tooth surface. It is the apical
extension of the crevicular gingival epithelium which is
not separated from the tooth surface (Smith, 1969). The
superficial cells form an area of attachment to the tooth
surface and may be attached to the enamel, dentine or
cementum (Listgarten, 1966). Between the superficial cells
and the tooth surface, a thin granular layer with an
average thickness of 800 Å is always present (Smith, 1969).
This attachment mode of the epithelium to calcified tissue
is unique and of biological importance. Because it is in
the form of a cementing substance, it is not a physical
continuity of structure (Smith, 1969). The nature of
attachment is that of glue rather than fibrous insertion
(Smith, 1969). The attachment is dynamic because its
strong adherence is maintained while the cells move. The
epithelial cells are fixed to the basement membrane by
hemidesmosomes. The cells of the attached epithelial cuff

are capable of DNA synthesis and mitosis and are constantly
dividing and exfoliating into the gingival crevice. Loe
(1967) stated that fluid only passes into the gingival
crevice from surrounding soft tissue in pathological
conditions, and the absence of tissue fluid from the
crevice is the best clinical indication of gingival health.

Connective tissues of the periodontium

The periodontium attaches the teeth to the jaw bone
and with use of the periodontal ligament allows teeth to
adjust their position when under stress (Melcher and
Eastone, 1969). The hard connective tissues of the
periodontium are bone, the alveolar process and cementum;
the soft connective tissues are the periodontal ligament
and the lamina propria of the gingiva. Epithelium covers
both of the soft connective tissues. The periodontium is
attached to dentin by cementum and to the jaw bone by the
alveolar process (Melcher and Eastone, 1969). The general
mineralization process of bone will be discussed first,
including the cells involved. Then the alveolar process
and cementum will be covered followed by the periodontal
ligament and lamina propria.

Bone   Calcification, the mineralization process of
bones and teeth, is directed by specific cells which are
surrounded by an organic matrix. In mammalian calcified

tissues, the major calcium salt is hydroxyapatite (Vogel, 1976). Bone mineral consists of two distinct calcium phosphates: an amorphous and a crystalline apatite phase. The amorphous phase is deposited first as the precursor so mature bone has approximately 70% apatite and 30% amorphous phase (Vogel, 1976).

The hormones involved in systemic regulation of bone formation include parathyroid hormone, calcitonin and 1,25-dihydroxyvitamin D_3 (Marks and Popoff, 1988). Local regulation, however, is controlled by cytokines, growth factors and prostaglandins (Marks and Popoff, 1988).

The initiation of calcification can occur in two ways, homogeneous and heterogeneous nucleation, the second of which is more widely accepted (Vogel, 1976) In the heterogeneous nucleation process, the catalyst allows apatite to form from large metastable calcium and phosphate concentrations. In the homogeneous nucleations process, bone cells synthesize and secrete membrane-bound matrix vesicles into extracellular fluid to form the initial bone (Spence and Mason, 1987). After calcification is initiated, tissue is mineralized in the organic matrix. Water is lost and mineral is accumulated to change the amorphous calcium phosphate into apatite and to start growing crystals (Vogel, 1976).

The structural unit of mature compact bone is the osteon or Haversian system. The osteon has a central Haversian canal that is surrounded by layers of bone. Lacunae, small cavities, are located between adjacent lamellae. At least one blood capillary is located in the haversian canal. This supplies nutrition and removes waste.

The bone cells found on the surfaces and interior of bone are shown in Figure 3.
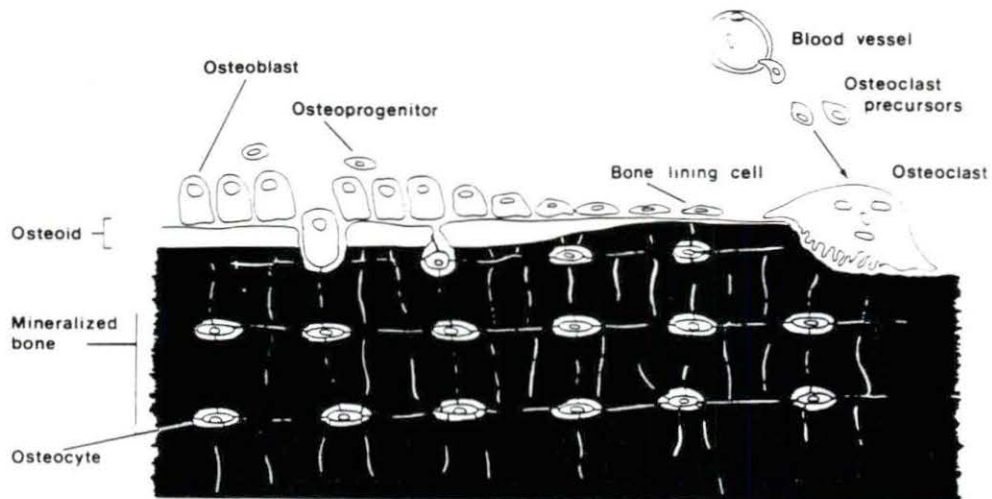
Figure 3.   Topographic relationship among bone cells
            (Marks and Popoff, 1988)

The bone cell responsible for the manufacture of bone is the osteoblast. The osteoblast is a transitional cell which is differentiated from a precursor cell to become active (Ranly, 1976). Its life time is limited, and it is not capable of mitosis when fully developed. The osteoblast is a surface cell found lining the bone with an osteoblastic layer which is one cell layer thick. The osteoblast can be in a variety of shapes, such as ovoid, columnar, and pyriform, depending on its developmental stage. Some osteoblasts get embedded as they are laid down and then become osteocytes. When active, the osteoblastic cell is highly polarized and has its nucleus distant from the bone matrix; on the contrary, when it is inactive, it is a thin, squamous-like cell with a flattened nucleus at the center of the cell. Anatomically, the osteoblast is described as being mononucleated, with an elaborate endoplasmic reticulum, well-developed Golgi-apparatus and numerous mitochondria (Banks, 1986). The osteoblast synthesizes and secretes type I collagen and initiates the calcification process (Marks and Popoff, 1988). Osteoblasts are stimulated by two driving forces for remodelling, mechanical and metabolic (Ranly, 1976). The mechanical stimulations are forces on the bone which lead to the generation of an electrical event, which in turn

triggers a chemical change. On the other hand, metabolic stimulation is triggered by a need for blood calcium and involves hormones.

The osteocytes are osteoblasts which have been embedded by their products of secretion so that the interstitial substance becomes mineralized (Banks, 1986). They exist in the bone tissue in lacunae of the osteon and exhibit numerous cytoplasmic projections. The tiny protoplasmic processes of osteocytes touch surface osteoblasts and the processes of other osteocytes located in adjacent lacunae (Ranly, 1976). All of the lacunae within each haversian system are interconnected by canniculi, tiny canals. Osteocytes vary in size, shape, and organelle content (Ranly, 1976). Osteocytes can make and resorb bone in order to homeostatically maintain blood calcium levels (Banks, 1986) and are therefore responsible for minute-to-minute control of plasma calcium (Ranly, 1976) The lifespan of some osteocytes can be many years after which they degenerate (Ranly, 1976). The osteocytes are stimulated by parathormone and Vitamin D (Ranly, 1976).

The osteoclast is the bone cell responsible for resorption of mineralized bone and cartilage. This cell is a multinucleated giant cell, moderate to large in size, with a brush border (Ranly, 1976). It has been measured to

be 85 µm by 105 µm in size making it one of the largest
cells in the body (Ranly, 1976). The osteoclasts reside on
the surfaces of bone in concavities called Howship's
lacunae (Banks, 1986). Osteoclasia, the process of bone
removal, occurs at the junction of the fingerlike
projections of the brush border and the bone (Ranly, 1976).
Osteoclasts are not capable of mitosis and are derived from
macrophages (Banks, 1986). They have a brief life span of
approximately one week (Ranly, 1976). The bone resorption
process is accomplished by releasing organic acid to
demineralize the bone (Banks, 1986). Collagenase,
proteases and hyaluronidase remove the matrix, while
lysosomal enzymes remove the cells (Ranly, 1976).
Osteoclasts are stimulated indirectly by chemical agents
such as parathyroid hormone, Vitamin D_3 and prostaglandin E
and by mechanical forces (Ranly, 1976).

Alveolar process   The alveolar process is an
integral part of the maxilla and the mandible and surrounds
the roots of the teeth, extends between them and is in
immediate contact with the periodontal membrane (Melcher
and Eastone, 1969). However, the junction between the
alveolar process and the jaw bone cannot be defined. The
alveolar process is divided into two parts: the alveolar
bone, to which the fibers of the periodontal ligament are

attached, and the supporting bone, which comprises the outer cortical plate and cancellous bone (Melcher and Eastone, 1969). The alveolar bone is an immature bone in which the collagen fibers are not arranged in typical lamellar patterns present in adult bone. Vessels and nerves perforate the alveolar bone to supply the soft connective tissue.

Cementum   Cementum, a liable tissue, is firmly attached to the dentin of the tooth to maintain a close contact between the tooth root and the sockets (Melcher and Eastone, 1969). Cementum extends from the cervical limits of the enamel to the apex of the root. Peripherally, cementum is contiguous with the soft connective tissue of the periodontal ligament and the gingival lamina propria, therefore providing attachment for some of their fibers. The cementum is the least hard of the hard connective tissue, yet it has some of the same properties as bone (Melcher and Eastone, 1969). Even though cementum is similar to bone, it has no haversian systems and blood vessels. The cells of cementum, cementocytes, have an appearance like osteocytes and are responsible for mineralization of cementum (Vogel, 1976). Cementum keeps depositing throughout life and therefore varies in thickness (Melcher and Eastone, 1969). Kronfeld (1931)

found the thickness of cementum to be 10 μm in the neck portion and 600 μm in the apical region, adding that deposition does not depend on function.

Periodontal ligament   The periodontal ligament, also called the periodontal membrane, is located between the cementum and the alveolar bones to fix the teeth in the bone sockets.   It is basically composed of collagen fibers which are attached to the cementum of the tooth and to the bone tissue of the socket (Ranly, 1976)   At the tooth neck it merges into the lamina propria of the gingiva.   It is described as the soft connective tissue that extends between the cementum and the alveolar bone and serves as the periosteum to alveolar bone (Melcher and Eastone, 1969).   The functions of the periodontal ligament are support, nutrition, formation and removal of tissue (Melcher and Eastone, 1969).   The fibers of the periodontal ligament are embedded in cementum and in the bone lining the sockets of the teeth.   The space between the fibers is filled with glycosaminoglycans (Junqueria and Carneiro, 1980).   The periodontal ligament space is widest at the tooth neck and cervically, yet apically it is wider than at mid-root (Kronfeld, 1931; Coolidge, 1937).   The width of the periodontal ligament depends on the load carried by the tooth in function.   A narrow periodontal ligament is found

when dental function is decreased, but the average width of the periodontal ligament is about 0.2 mm (Melcher and Eastone, 1969). The tooth function also affects the quantity and caliber of fiber bundles in the periodontal ligament, and as tooth function increases there is an increase in fiber development (Melcher and Eastone, 1969).

Lamina propria   The lamina propria of the gingiva is connective tissue which is continuous with the periodontal ligament. Anatomically, it is divided into two regions: attached gingiva, which covers the alveolar bone and the cementum, and the marginal gingiva, which covers the neck portion of the teeth (Melcher and Eastone, 1969). The lamina propria is limited by the epithelium lining the gingival crevice of the epithelium, the attached epithelial cuff, cementum, periodontal ligament, alveolar bone, connective tissue of the alveolar mucosa and the masticatory epithelium (Melcher and Eastone, 1969).

Implant Design

The function of an endosseous tooth root implant is to replace a tooth. It is inserted into the site of the missing or extracted tooth in order to restore the original function. Because dental implants must be transcutaneous to be functional and are therefore exposed to the hostile

oral environment, tooth replacement is a challenging problem (Park, 1987).

To design a successful implant, a number of factors must be considered. First, the implant material must be chosen to fit the mechanical and chemical requirements of the original, natural element which is being replaced. Second, the implant shape must be designed to meet the physical requirements. Finally, because of the definite effect of surface structure on tissue ingrowth, consideration must be given to the type of surface.

Materials

Metal, ceramic, plastic and composite materials are used for dental implants. A comprehensive list of the various materials used as dental implant tests is given by Natiella (1986).

All of these materials must meet the material requirements for the success of long-term functional endosseous implants (Grenoble and Voss, 1976):

1. The material should not chemically irritate the tissue or cause resorption of the supporting bone and should be well tolerated by oral tissues,

2. The material must maintain its mechanical properties in the oral environment for long term

applications by having sufficient corrosion resistance to physiological and oral fluids,

3. The material should develop an effective bacterial seal between the implant and the mucosal tissues to prevent infection.

Consequently, biocompatibility, which is the degree of tissue response toward the material, is a basic biological property critical to the success of the material. Another property of the material to be considered is its surface energy. High-surface energy materials have been found to have three times more fibroblastic-fibrocytic cells adjacent to the implant material to produce bonding with it, whereas the low-surface energy materials were walled-off by a capsule (Baier et al., 1984). Consideration of this property is more important in the selection of metals due to the high-surface energy caused by the cleaning treatment and oxide layer formation.

The materials' mechanical properties are important aspects in implant design because the biomaterial and design can control the interfacial interactions (Lemons, 1983). Brunski (1988a) stated that the relationship between biology and mechanics should be central to dental implant design and lists these biomechanical issues:

- mechanical loading on the implant *in-vivo*

- transmission of the loadings to interfacial tissues,

- and biological reactions of the interfacial tissues
   to the transmitted loadings.

Analyses have shown that bone exists within a stress
envelope: if stress is too low, bone resorbs, However if
the stress is too high, destruction and resorption occurs
(Hassler et al., 1983). Hassler et al. (1983) studied
static loads in rabbit calvarium and extrapolated the data
to alveolar bone. He found that 30-350 psi static load
allows remodeling rates of the surrounding bone to exceed
control levels.

Lemons (1983) proposed that mechanical transfer of
force at the microscopic level along the biomaterial
interface is quantitatively related to the modulus of
elasticity of the biomaterial and the tissue. Figure 4
gives the stress-strain values for several biomaterials and
biological tissues. This graph shows that ceramics and
metals are a lot stiffer than bone and skin. Of importance
to implant design is the area of force transfer involved in
mechanical stress (Lemons, 1983). The higher the area of
contact between the tissue and material, the lower the
stress magnitude at the bone/material interface. This
concept also applies to soft tissue adjacent to a
percutaneous device. Forces applied to the device or the
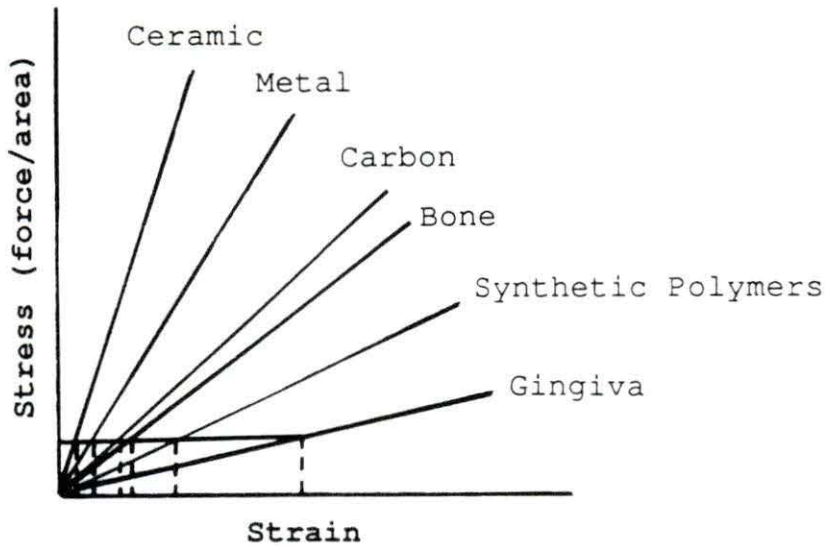
Figure 4.   Stress versus strain relationship for selected
             biomaterials and tissues (Lemons, 1983)

skin adjacent to the implant can result in tearing of the

interface due to the gross difference between the modulus

of elasticity of the two materials (Hall et al., 1984).

Shape

A variety of dental implant shapes has been designed

and tested: screws, pins, blades, cylinders, frameworks or

combinations of two designs (Natiella, 1986).   Because the

duplication of the natural tooth support system using

artificial devices is impossible, emphasis has been placed

on designing a long-term functional implant (Natiella,

1986).   In the last 60 years, three types of implant shapes

have been developed and are currently still popular: the subperiosteal, the blade and the root form or cylindrical shape (Balkin, 1988).

Research to determine the effect of implant shape on tissue response has been done in two ways: theoretically by using finite element stress analysis and clinically by observing cellular behavior. Atmaran et al. (1979a) tested three different geometries of ankylosed single-tooth implants: conical, natural tooth and cylindrical. The results showed that a cylindrically-shaped implant produces the least amount of stresses in both the implant and the mandible. In an additional study Atmaran et al. (1979b) examined the effect of the implant root length and found that a longer implant root generally resulted in an insignificant reduction of maximum stresses both on the implant and the alveolar bone.

Matlaga et al. (1976) found that the implant shape had a definite effect on the cell population, metabolism and turnover. Because the success of any biomaterial implant depends on the cellular behavior at the implant/tissue interface, shape characteristics must be taken into account since they can modify cellular response (Salthouse and Matlaga, 1983). In a study done by Salthouse and Matlaga (1983), three cross-sectional configurations, cylinder,

triangle and pentagon, with the same surface area per unit
length, were implanted and evaluated for lysosomal enzyme
activity associated with the implant sites by using
microspectrophotometry. Results demonstrated the lowest
activity with circular rod samples and highest activity
with triangular samples, which is probably due to damage
caused by the latter shape. Lysosomal enzyme activity had
previously been found to be a reasonable, objective measure
of implant tissue reactivity (Salthouse and Matlaga, 1975).
The conclusion drawn from this experiment is that smooth
contoured implants without sharp angles are more acceptable
to the tissue.

Surface topography

Numerous researchers have investigated the effects of
surface topography on tissue response: however,
contradictory results have been reported. For dental
implants, the tissues involved are bone and the gingival
epithelium.

Some researchers found that surface structure had no
effect on bone response. Freeman (1972) concluded that the
surface finish of titanium implants, ranging from a rough
surface to a smooth surface texture, seemed to have little,
if any effect on the mandibular tissue response. Van
Blitterswijk et al. (1985) investigated dense and

macroporous hydroxyapatite implanted in the middle ears of rats and saw no distinct difference between the two surfaces with respect to the bone tissue/implant interface.

However, most researchers think that surface topography of the implant materials does affect the adjacent tissue and can be designed to facilitate the reaction of different types of tissues. In the past, theories about the critical pore size for bone development have been in the range of 75-150 μm (Natiella, 1986), but varying results have disputed that. In one study experimenters implanted material with pores 20 μm in diameter and 75 μm deep and found mineralized tissue formation in the pores (Ehrnford et al., 1980).

The formation of a mucosal seal, the attachment mechanism of the gingival epithelium to the implant post which projects into the oral cavity, is critical for the long-term success of the implant device. Failure to obtain this seal allows the leakage of toxins and antigenic material into the underlying tissue, which results in inflammation and tissue destruction (Collins and Squier, 1980). Recently, a lot of attention has been placed on the soft tissue attachment to materials with varying surface topographies. Often, research is being done using *in-vitro* cell attachment experiments to determine preliminary

findings before turning to animal studies. Human gingival explant cells were cultured on grooved titanium-coated silicon wafers and were able to be guided by the topography, therefore, controlling the direction of cell migration (Brunette et al., 1983).

In the normal wound healing process of epithelium surrounding all percutaneous implants, the tissue retracts due to scar tissue formation (Hall et al., 1984). To keep the implant from failing, continued downgrowth of the epithelium must be prevented. To study this process, Squier et al. (1988) implanted varying pore sized millipore filters in the backs of pigs. Filters with pore sizes of 3-8 µm allowed collagen fibril formation within the interstices, consequently stabilizing downgrowth after the first week to form a relatively stable junction. Another study, examining soft tissue response by varying both pore size or material, reported minimal tissue response for 1 and 3 µm pore sizes, and no fibrous attachment for a surface roughness of larger than 10 µm (Campbell and von Recum, 1989).

Cellular behavior adjacent to the implant surface is indicative of the type of tissue response. For example, the macrophage is a major phagocytic cell and the component in the cellular response to foreign bodies (Salthouse,

1984). Salthouse and Matlaga (1983) studied the macrophage activity at rough and smooth surfaces and concluded that the macrophage populations were several fold higher on the rougher surface even after 90 days of implantation. He recommends using smooth implants to obtain better biocompatibility characteristics.

Current Status of Dental Implants

The materials which are being used as dental implants in clinical practice and research include metals, ceramics, polymers. Table 2 lists the implant materials to be discussed here. Composites are combinations of two or more of these materials and will be discussed in the respective section depending on the surface material or the main component of the composite.

Metals

For metal implants, stainless steel, cobalt-chromium-molybdenum alloys, titanium, and titanium-aluminum-vanadium (Ti-6Al-4V) alloys are currently being used as dental implant materials in the United States, Europe and Japan (Worthington, 1988). Implanted stainless steels cannot resist all forms of corrosion attack evident in a biological environment, so stainless steels are mainly used as a core material (Williams, 1981). Klawitter et al.

Table 2. Categories of materials used for dental
          implants (Hulbert et al., 1987)

Category	Subdivision	Material
Metals		stainless steel cobalt-chromium-molybdenum alloy titanium Ti-6Al-4V
Ceramics	Nearly inert	alumina LTI carbon ULTI carbon vitreous carbon
	Surface active	glass glass-ceramic hydroxyapatite
	Resorbable	calcium sulfate trisodium phosphate calcium and phosphate salts
Polymers		polyethylene polymethylmethacrylate ultra-high molecular weight polyethylene

(1975) found only a 41% success rate for cobalt chromium-
molybdenum alloy implants in dogs even though they did
observe tissue ingrowth into the implant material.
However, there is concern about the general toxicity of the
individual elements of this alloy, cobalt, chromium and
molybdenum (Williams, 1981). Further, Grenoble and Voss
(1976) reported that cobalt-chromium alloys are not well

tolerated by oral tissues and form a relatively thick membrane around the implant.

Pure titanium metal implants have shown excellent biocompatibility as an endosseous dental implant (Williams, 1981) and have integrated into the host tissue (Hannson et al., 1983). Branemark et al. (1969) have done extensive studies of titanium and reported no undesired reaction of the bone or adjacent soft tissue of titanium implants in a 5-year implants study in dogs. Later, the same research facility found the implants to be surrounded by hard and soft tissues, which stayed healthy for up to 15 years in humans (Adell et al., 1981). On the contrary, Grenoble and Voss (1976) stated that fibrous tissue encapsulation of titanium implants has been found.

By alloying titanium, the mechanical properties of the metal can be improved. Ti-6Al-4V is an example of such an alloy. The Core-Vent® implant, made from the Ti-6Al-4V, has a reported success rate of 98% (Niznick, 1985). Recently however, investigations found that the alloy could be a localized source of the aluminum and vanadium elements (Bruneel and Helsen, 1988) Because of the adverse reactions of metal implants more emphasis is now being placed in coating these implants with a ceramic or polymer to make a composite.

Ceramics

Alumina, both polycrystalline and single crystal, phosphates, carbons and bioglass have been tested as dental implant materials. These materials have been divided into three categories according to their biological activity and response from living tissue. Figure 5 shows the relative reactivity times for these bioceramic materials.
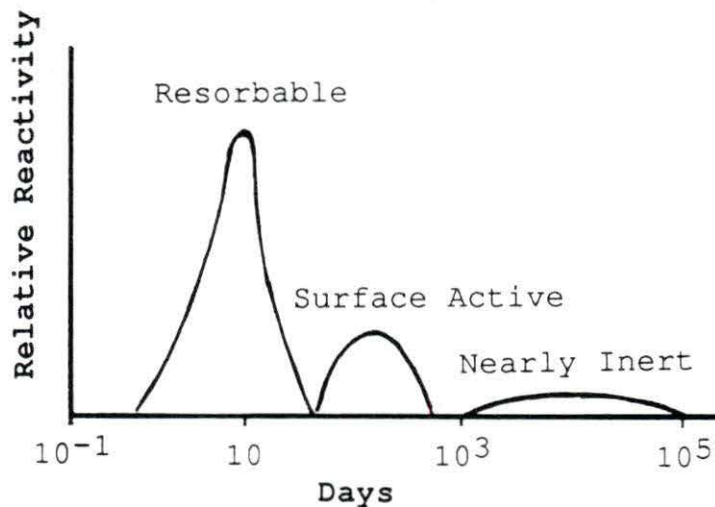
Figure 5.   Relative reactivity for bioceramic materials (de Groot, 1981)

Nearly inert ceramics   Nearly inert ceramics include various carbons and alumina. Used in Europe since 1966, alumina, the abbreviation for aluminum oxide (Al_2O_3), is mostly used as a high purity (99.9%), dense, polycrystalline compound. When it is highly polished, alumina has a exceptionally low coefficient of friction and

also low wear resistance in a physiological environment (Hulbert et al., 1987). Heimke et al. (1987) reported its large scale applications for load-bearing dental implants following good histological results from a three year animal study. In 1985, Boretos stated that over 60,000 successful dental implants made of alumina had been performed over the past 10 years. Another crystal structure of alumina used for dental study, single crystal α-alumina, has been tested in animals and is being used in human dentistry. McKinney et al. (1985) reported a success rate of 94.5% in a five year implant study and found evidence for the presence of a permucosal seal at the tissue/implant interface.

Carbon, another inert material, has a crystal structure which can be varied to achieve a variety of properties. Low Temperature Isotropic (LTI) and vitreous carbon are both applicable as dental implant materials. LTI carbon has been found to be biocompatible, but its use as a dental implant has received mixed results and is therefore awaiting design improvements (Hulbert et al., 1987). Vitreous carbon tooth root replacements combine a stainless steel core with a carbon implant. Some devices have been found to contain fractures through the carbon

causing the manufacturer to eliminate the damaged implants (Lemons et al., 1988).

Surface-active ceramics   The surface active bioceramics include glass, glass-ceramic and hydroxyapatite. One of the most famous bioceramic glasses is Bioglass® developed by Hench. This material was the first to show evidence of direct bone bonding to an implant material (Hulbert et al., 1987). It has been used as a tooth root implant, but its applications are limited to devices where strength is not a factor since it is inherently weak (Boretos, 1985). Cerevital, a similar version of Bioglass, has been used in Europe.

Another material in the surface-active classification is hydroxyapatite, $Ca_{10}(PO_4)_6OH_2$. It has been shown to allow direct bone bonding to the material (Jarcho, 1986). Due to its loss of strength from resorption, hydroxyapatite has been used to coat metal, therefore endowing the implant with surface activity while getting strength from the metal. The coating has been applied to the surface of titanium and cobalt based alloys to provide opportunities for tissue integration (Lemons et al., 1988). Kent et al. (1990) have just reported an overall success rate of 95% in a 5-year, 772 human implant study of hydroxyapatite coated titanium implants. Even though there have been problems

with failure of prosthetic devices due to the hydroxyapatite coating shearing off the base metal or metal alloy (Cook and Thomas, 1990), Kent et al. (1990) did not observe failure of the hydroxyapatite/metal interface. Hydroxyapatite and other calcium phosphates have shown excellent biocompatibility and will be discussed in detail in the following section calcium phosphate as a biomaterial.

Resorbable ceramics   The calcium and phosphate salts, trisodium phosphate and the calcium sulfates are in the resorbable bioceramic category. Calcium sulfates, or plaster of Paris, was one of the first resorbable materials to be used as a scaffold for bone, but due to its unpredictable rate of absorption it is not used much presently (Boretos, 1985). Trisodium phosphate however, has bone forming abilities when coated with autogenous bone (McDavid et al., 1979).

The calcium and phosphate salts make up the major portion of the resorbable ceramics. The ratio of calcium/phosphate varies from 1:2 to 2:1, named monocalcium phosphate and tetracalcium phosphate, respectively. Of these, the main material being presently used is tricalcium phosphate with a Ca/P ratio of 3:2 (Hulbert et al., 1987).

Polymers   The most common polymers used for dental implants are polyethylene and polymethylmethacrylate. Richardson et al. (1975) tested ultra-high molecular weight polyethylene (UHMWPE) and found fibrous tissue adherence to this to be higher than to other implant materials being tested. Klawitter et al. (1975) implanted polymethylmethacrylate implants with porous roots and found bone and fibrous tissue growth into pores of specific sizes.

Calcium Phosphates as Biomaterials

Calcium phosphates are applicable as biomaterials because of their exceptional biocompatibility. This is due to the calcium and phosphate ions, which are the most common components of hard tissue. The main constituent of hard tissue is calcium hydroxyapatite, but other calcium salts, such as octacalcium phosphate, monetite [$CaH(PO_4)$], brushite [$CaHPO_4 \cdot 2H_2O$], amorphous calcium phosphate, calcium pyrophosphate and tricalcium phosphate, are also present in the early development of hard tissues or in the later developmental stages (de Groot, 1981). The calcium phosphates can be categorized according to their Ca/P ratios, and the principal calcium salts of orthophosphoric acid are listed in Table 3.

Table 3. Principal calcium salts of orthophosphoric acid
(Heughebaert and Bonel, 1986)

Symbol	Chemical Formula	Chemical Name	Ca/P Ratio
DCPD	$CaHPO_4$ $2H_2O$	dicalcium phosphate dihydrate	1.00
DCPA	$CaPO_4$	dicalcium phosphate anhydrous	1.00
OCP	$Ca_4H(PO_4)_3$ 2.5 H_2O	octacalcium phosphate	1.33
TCP	$Ca_3(PO_4)_2$	tricalcium phosphate	1.50
HAP	$Ca_5(PO_4)_3$ (OH)	hydroxyapatite	1.67
TCPM	Ca_4 P_2O_9	tetracalcium phosphate	2.00

In general, calcium phosphates have been found to be one of the most biocompatible hard tissue implant materials for several reasons (Jarcho, 1986):

· no local or systemic toxicity,

· no inflammatory or foreign body responses,

· integration with natural bone without encapsulation by fibrous tissue,

· no alteration of normal bone mineralization process,

· and strong bond with living bone.

Of the calcium phosphates, the two compounds which have been studied more extensively are hydroxyapatite and tricalcium phosphate. First hydroxyapatite, then

tricalcium phosphate, will be discussed with regard to their chemical, biological and mechanical properties. Finally, a composite of calcium phosphate and spinel will be reviewed.

Hydroxyapatite

As shown in Table 3, the chemical formula for hydroxyapatite (HAP) is $Ca_{10}(PO_4)_6(OH)_2$ giving it a Ca/P ratio of 1.67. In an anhydrous system, HAP is not stable due to this chemical reaction (de Groot, 1980):

$$Ca_{10}(PO_4)_6(OH)_2 \rightarrow 2Ca_3(PO_4)_2 + Ca_4P_2O_9 + H_2O$$
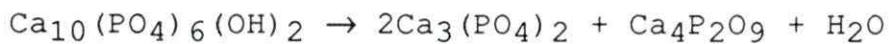
A dynamic equilibrium between HAP, other calcium phosphate salts and serum exists as follows (de Groot, 1981):
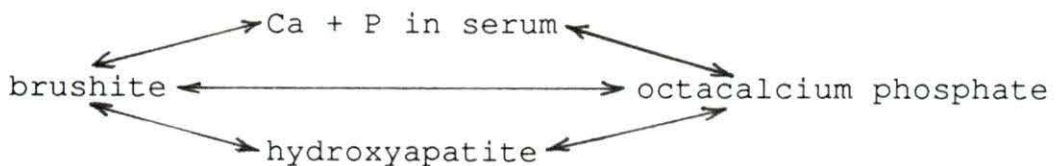
After implantation of HAP, this interaction occurs with body fluid. The crystal structure of HAP, like other members of the apatite family is a hexagonal rhombic prism (Park, 1987). HAP in many cases has a deficit of calcium, making its chemical formula $Ca_{10-x}H_{2x}(PO_4)_6(OH)_2$ (Naray-Szabo, 1969). The missing calcium atoms are then replaced by hydrogen bridges.

The biocompatibility of HAPs as hard and soft tissue implants has been well documented. Denissen et al. (1980) was one of the first to propose that a chemical bond developed between bone and ceramic. The HAP provides a physical matrix for new bone deposition and has therefore been described as being osteoconductive or osteophilic (Jarcho, 1986). As a soft tissue implant, hydroxyapatite has been found to be compatible in epithelial, connective, periosteal and dermal applications (de Groot et al., 1988).

Biodegradation or resorbability of calcium phosphates affect their mechanical and biological properties as a biomaterial. These properties are controlled by the chemical constitution and the microstructure or porosity (de Groot, 1981). For example, high density ceramics have less surface area and therefore a lesser tendency to undergo bioresorption. Jarcho et al. (1976) found little or no degradation after a 6 month implant period of dense, polycrystalline hydroxyapatite. This was confirmed by Denissen et al. (1979) who implanted dense HAP and found no measurable degradation after one year. Consequently, Jarcho (1986) has defined dense HAP as non-resorbable. Figure 6 shows solubility isotherms for several calcium phosphates as a function of pH. From this it can be seen that HAP is the most stable phase under many conditions.
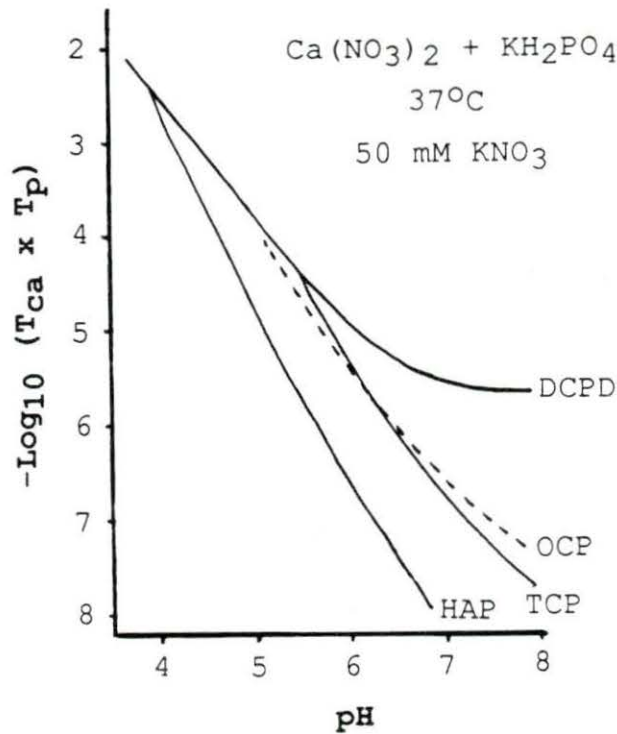
Figure 6.   Solubility isotherms for calcium phosphates as
             a function of pH (Heughebaert and Bonel, 1986)

LeGeros et al. (1988) suggested the following relationship

between the biodegradation of HAP and tricalcium phosphate:

$$\alpha\text{-TCP} > \beta\text{-TCP} >>> \text{HAP}$$
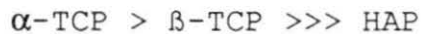
Like all ceramic materials, the mechanical properties

of HAP are stronger in compression than in tension. Jarcho

et al. (1976) reported a compression strength of 917 MPa, a

tensile strength of 196 MPa and a modulus of elasticity of 34.5 GPa for dense HAP. For comparison, strength values for cortical bone are 167 MPa in compression, 121 MPa in tension and an elastic modulus of 17.2 GPa (Park, 1984).

Tricalcium phosphates

Tricalcium phosphate (TCP) is any calcium phosphate with a Ca/P ratio of 1.5. Table 4 gives tricalcium phosphate compounds with their chemical formulas and structures. Of the TCP compounds listed in Table 4, the ß and α structures have been well defined, whereas the

Table 4. Pure tricalcium phosphates, Ca/P = 1.5
(Heughebaert and Bonel, 1986)

Symbol	Chemical Formula Mineral Name	Chemical Name (Temp. Range)
Am-TCP	$Ca_3(PO_4)_2$ + adsorbed H_2O	amorphous TCP
Ap-TCP	$Ca_3(HPO_4)(PO_4)_5(OH)$	apatitic TCP (t<100°C)
ß-TCP	$Ca_3(PO_4)_2$, ß phase whitlockite	anhydrous ß-TCP (t<1120°C)
α-TCP	$Ca_3(PO_4)_2$, α phase	anhydrous α-TCP (1120°C<t<1470°C)
HP-TCP	$Ca_3(PO_4)_2$, high pressure	high pressure TCP

apatitic TCP structure has only been roughly defined
(Heughebaert and Bonel, 1986).

Because TCP is unstable in water, it can't exist in
physiological conditions (de Groot, 1980). The reaction of
TCP with water is as follows:

$$H_2O + 4\ Ca_3(PO_4)_2 \rightarrow Ca_{10}(PO_4)_6(OH)_2 + 2Ca^{2+} + 2HPO_4{}^{2-}$$

So the surface of the TCP particles will actually become
HAP after being exposed to physiological fluid. De Groot
(1980) concluded that any particles with a Ca/P ratio
between 1 to 2 will have no biological differences in
interface behavior due to the above reaction.

The biocompatibility of TCP was shown by Cutright et
al. (1972). TCP cylinders implanted in the leg muscle of
rats were very well accepted by tissue, and bone deposited
directly against and within the cylinders. With regard to
the different crystallographic structures, both the α and ß
phases of TCP have been shown to be compatible with bone
(Ferraro, 1979, Cameron et al., 1977). Biodegradation of
TCP has been described by de Groot (1980) as being done
partially by a cellular mechanism where macrophages and
giant cells will consequently contain ceramic particles.
The biodegradation of ß-TCP and α-TCP is much higher than
HAP (LeGeros et al., 1988). Figure 5 shows the solubility

of TCP compared to other calcium phosphate compounds.
Similarly, Jarcho (1986) found TCP to dissolve 12.3 times
faster in an acidic and 22.3 times faster in a basic
environment than HAP. However, like HAP, these rates of
resorption are dependent on microporosity. In addition,
the host tissue affects the rates of resorption for TCP.
Klein et al. (1984) found substantially different
resorption rates for TCP between soft tissue and hard
tissue implants.

The mechanical properties of dense TCP were found to
be 687 MPa in compression, 154 MPa in tension and 33.0 GPa
elastic modulus (Jarcho et al., 1979). Because TCP is very
bioresorbable and is usually largely replaced by bone
(Cutright et al., 1972; de Groot, 1981), it acts as a
scaffold to stimulate bone growth. After resorption takes
place, mechanical properties decrease.

Tricalcium phosphate/spinel composite

As stated previously, tricalcium phosphate (TCP)
offers good biocompatibility but loses strength due to
biodegradation. By adding an inert material, the long
term-strength can be improved. Janikowski and McGee (1969)
first suggested whitlockite ($Ca_3(PO_4)_2$) and magnesium
aluminate spinel ($MgAl_2O_4$) to make artificial teeth with
low solubility.

Magnesium aluminate spinels have a face-centered cubic
close packed crystal structure. This spinel has a low
solubility in aqueous solutions (Janikowski and McGee,
1969). The hard and soft tissue biocompatibility of spinel
has been shown to be excellent when implanted in swine bone
with intimate tissue/implant interfacing (Karagianes et
al., 1976) In addition, comparison of spinel with alumina
and Ti-6Al-4V alloy found little difference in rate of
tissue ingrowth and no inflammatory response. Richardson
et al. (1975) found spinel disks to have a slightly better
compatibility than several other materials implanted in
muscle of rabbit.

By combining refractory spinel with calcium phosphate,
no reactions or mutual solid solutions are formed (McGee,
1974). McGee and Wood (1974) showed that sintering of a
composite mixture of calcium phosphate and magnesium
aluminate spinel consists of two phases with no
intermediate compounds. They termed the composite
osteoceramic, which will also be used in this project for
the tricalcium phosphate/spinel composite. When tooth
implants with dense and porous regions were submucosally
implanted in the mandible and maxilla of dogs, strong bone
attachment to the prosthesis with no indication of a
fibrous capsule was found (McGee and Wood, 1974). Tweden

(1987) compared four endosseous dental implants made of
single-crystal sapphire, pyrolytic carbon, Ti-6Al-4V alloy
and calcium phosphate/spinel composite (osteoceramic)
implanted in the mandibles of dogs. The tissue response of
the osteoceramic implant was found to be superior to that
of the three commercially-available implants.

The physical and chemical properties of the
osteoceramic were further studied by Graves (1988).
Results showed that the osteoceramic has a higher
compressive strength and tensile strength than cortical
bone and a modulus of elasticity similar to titanium. No
strength loss was observed after bars of the osteoceramic
material were exposed to Ringer's solution for 7 month,
therefore no strength degradation of the osteoceramic
composite was detected.

MATERIALS AND METHODS

The steps of this study were to design, implant and clinically evaluate a transgingival tooth root suitable for the canine mandible. In order to implant the tooth roots in dogs, the natural teeth were extracted first.

Tooth Extraction Procedure

Ten mongrel dogs representing both sexes were used for this implant study. Large mongrel dogs are the best model for human dental implant research, because they offer favorable characteristics for use in comparative studies (Cranin et al., 1988). The dogs weighed between 19 and 28 kg, with an average weight of 24.2 kg as shown in Table 5.

Table 5. Dog weights and sex

Dog Number	Weight (kg)	Sex
7934	24.5	F
8722	24.1	M
8724	25.0	F
8725	19.0	M
8730	25.0	M
8732	25.0	F
8733	25.0	M
8734	24.0	M
8736	22.7	F
8739	27.7	M

Anesthesia was induced using Surital®[1] (17.5 mg/kg) intravenously to effect and maintained using 1-2% halothane gas. Surital® is a thiamylal sodium solution which acts as an ultrashort barbiturate. Atropine sulfate[2] (0.5 mg/kg) was administered subcutaneously to all dogs as a cholinergic blocking agent to increase the pulse rate. In one dog, Dopram®[3], a doxapram which acts as an adrenergic agent (5 mg/kg), was given as a respiratory stimulant. Radiographs of both sides of the mandible were taken prior to extraction. The 2nd, 3rd, and 4th mandibular premolars were extracted bilaterally. To help extract the roots individually, the crowns were separated by cutting them in half buccal-lingually with a dental diamond rotary saw. Some of the tooth root tips broke off during extraction and had to be drilled out with a dental bur. The width and height of the alveolar ridge, the thickness of the gingiva, as well as the length of the extracted roots were measured. The oral health of the animal, especially the gingival

---

[1]Parke-Davis, Warner-Lambert Co., Morris Plains, NJ.

[2]Fort Dodge Laboratories, Inc., Fort Dodge, IA.

[3]A. H. Robins Company, Richmond, VA.

condition, was noted. Penicillin G procaine[4] (0.1 ml/kg) was injected subcutaneously as an antibacterial agent. No food was given for at least 24 hours after the extraction procedure, at which time soft food was given for two weeks, followed by a standard hard diet. The mandibles were allowed to heal for at least 3 months.

Design of the Tooth Root Implant

Anatomical measurements

To aid in designing a good fitting tooth root, anatomical measurements were taken at the time of the tooth extraction procedure. The anatomical measurements taken in-vivo consisted of the sagittal width of the alveolar ridge, the height of the alveolar ridge between the original tooth positions and the thickness of the gingiva. The extracted teeth were measured to obtain the lengths of the tooth roots below the gingival attachment line. In order to accommodate the implant design in all ten dogs, the smallest anatomical measurements were used to construct the design.

_____

[4]Pfizer, Inc., New York.

Physical dimensions of the implant

In the surgical procedure to place these implants, it was necessary to cover the implants with a gingival flap to prevent infection during the healing process. After healing, the gingiva was cut back to expose the implant. Therefore, the shoulder height during the healing period must be low enough to allow gingival covering yet high enough to keep the gingiva from growing back over after it has been cut back. The implants were placed in drilled holes in the mandibular alveolar bone of the 2nd, 3rd, and 4th premolar region. Figure 7 shows the implant placement in the canine mandible.
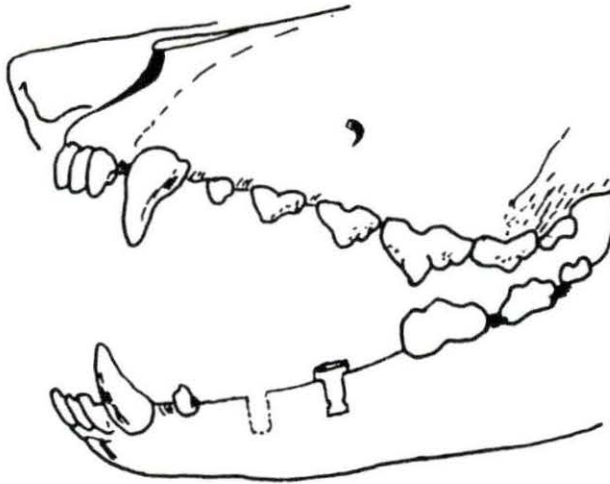
Figure 7.   Implant placement in the 2nd-4th premolar region of the canine mandible

Being slightly larger in diameter than the main shaft of the implant, the shoulder acted as a stopping mechanism to assure depth placement of the implant in the bone and to position the various surface structures of the shoulder adjacent to the gingiva. As a result, the physical considerations of the implant design which were important included shaft diameter, shaft length, groove, shoulder width and shoulder height of the implant.

A cylindrical implant shape was chosen because this shape has been found to have favorable stress distribution in bone (Atmaran et al., 1979a) and because it causes minimal cellular activity (Salthouse and Matlaga, 1983). From the anatomical measurements, the minimal width of the alveolar ridge including the mucosa was measured to be 6.9 mm and the width of the gingiva measured to be 1.5 mm; this makes the lingual-buccal width of the alveolar bone at least 5.4 mm. Therefore, a shaft diameter of 3.5 mm was determined to be adequate to assure bone stability around the top of the implant where the alveolar bone narrows. For the shortest tooth root, a value of 7.87 mm was measured. Consequently, the implant length of 7 mm below the shoulder was chosen so that the intermedullary canal would not be penetrated.

A previous study by Tweden (1987) found that a groove in the bottom portion of the implant allowed bone ingrowth for additional mechanical support. A groove diameter of 2.88 mm was used for the design. One of the functions of the shoulder width was to control the depth of implant placement by making the shoulder a stopping mechanism. The drill bits used for drilling holes in the bone have increments of 0.2 mm; therefore, a 0.5 mm shoulder width larger than the shaft diameter was determined to be adequate. The gingiva was measured to be between 1.0 mm and 2.5 mm thick. Similarly, the shoulder height should be at least 1 mm to match the gingival thickness. If the gingiva is loosened, it can be stretched easily, so 2, 3, and 4 mm shoulder heights were tried. The design of the implant with varying shoulder heights is shown in Figure 8.

Manufacture of the Implant

Tooth root implant

The ceramic tooth root was made using two raw material powders: calcium phosphate tribasic (Mallinckrodt) and magnesium aluminate spinel (Baikowski International Corp.). The spinel was a single calcined, high purity powder with a chemical composition of $MgAl_2O_4$. It had a true density of
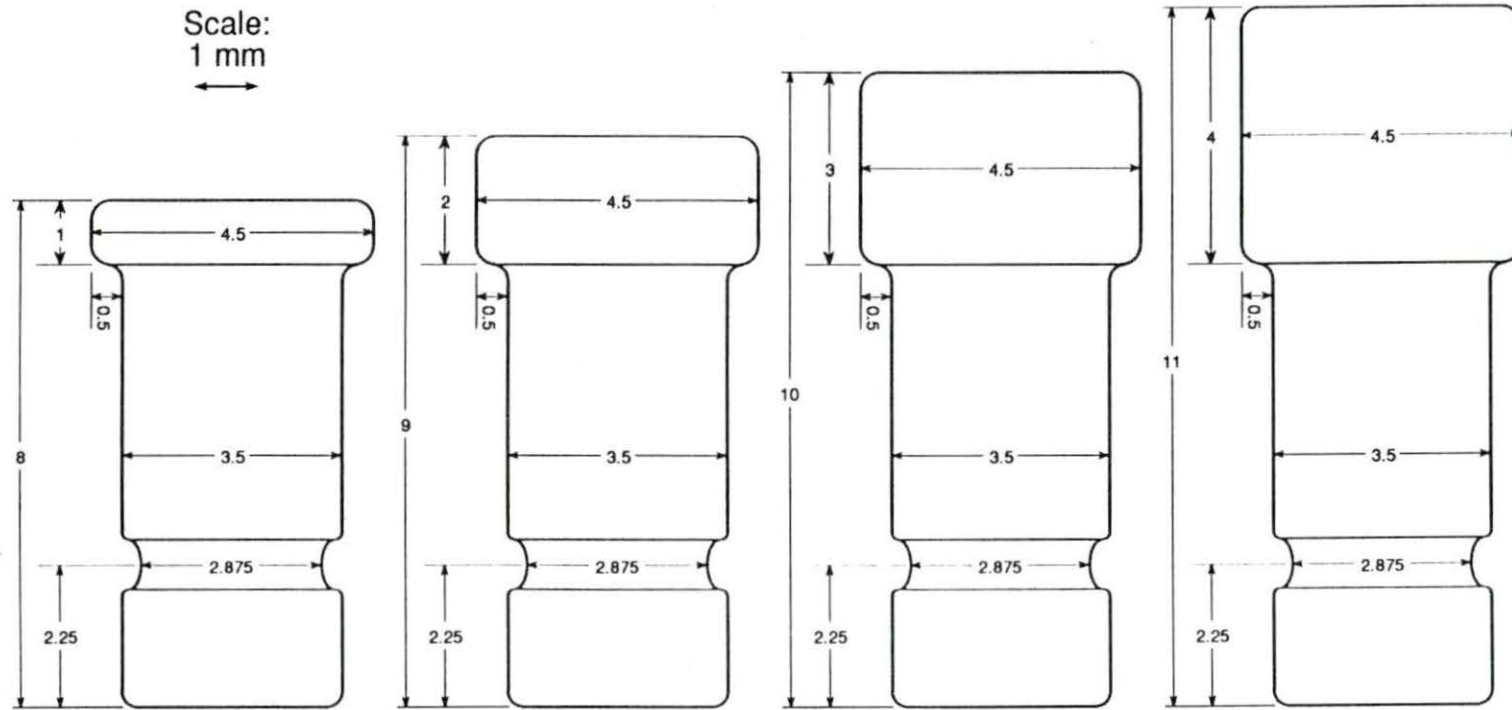
Figure 8. Implant design showing shoulder heights of 1, 2, 3, and 4 mm

3.57 g/cm^3 and an elementary particle size of 0.03 μm. The calcium phosphate tribasic has an approximate chemical composition of $Ca_{10}(PO_4)_6(OH)_2$ and a true density of 3.14 g/cm^3.

The ceramic composite was prepared by using 50 vol% calcium phosphate tribasic and 50 vol% magnesium aluminate spinel. To determine the required weights of the two powders, the equivalent volumes were multiplied by the true denstities of the powders. The raw materials were weighed out and dry stirred. A 9% binder/plasticizer solution was added to increase the green strength of the ceramic. The binder, 40303.00 Dow experimental binder[5], and the plasticizer, Polyglycol E-400 plasticizer[5], were mixed at a ratio of 20:1, respectively. Then 1.5% binder/plasticizer and 7.5% water were mixed together to make up the 9% binder/plasticizer solution. This solution was added dropwise to the powders and mixed thoroughly using a mortar and pestle. The mixture was then passed through a 30 Mesh stainless steel sieve. The mixing and screening step was repeated once again to assure thorough mixing. This resulted in an agglomerate particle size of smaller than 600 μm.

---

[5]Dow Chemical, Midland, MI.

Cylindrical pellets with a diameter of 1.27 cm and a length of about 2.54 cm were pressed from 4 g of ceramic powder using a Model C Carver laboratory press at a pressure of 4000 psi. The pellets were then isostatically pressed to 25,000 psi. The pellets were prefired to 1200°C at a heating and cooling rate of 150°C/hr in a silicon carbide resistance furnace. At this stage, the pellets were machined to the specific implant design, taking shrinkage values between 1200°C and 1450°C into account. The final step was to sinter the implants to 1450°C at a heating rate of 100°C/hr and a cooling rate of 150°C/hr.

Surface variations

As stated in the literature review, varying results concerning the effect of pore size on epithelial attachment have been found. Therefore, the shoulder surfaces of the implants adjacent to the gingiva were produced with three surface structures: (1) smooth with micropores, (2) slightly irregular, and (3) roughened with macropores and micropores. The purpose of this variation was to test the effect of surface structure on tissue adherence.

Smooth   To obtain a smooth ceramic surface, polishing was used. The shoulders of the tooth roots were

polished at low speed on a mineralogy polishing wheel using the following grit sizes and time periods:

600 grit silicon carbide for five minutes,

6 μm diamond paste for two minutes and

1 μm diamond paste for two minutes.

After each polishing cycle the implants were ultrasonically cleaned; then they were fired to 500°C to remove any residue.

Irregular   The as fired surface of the ceramic material produces an irregular surface with grains of ceramic material melted together. No further treatment was needed to produce the desired slightly irregular surface structure.

Rough   Since the ceramic composite consists of two phases, a soft tricalcium phosphate and a hard magnesium aluminate spinel, the soft phase can be etched out to create surface pores. Pore sizes of about 3-8 μm have been shown to be effective in allowing epithelial attachment (Squier et al., 1988) and producing minimal tissue response (Campbell and von Recum, 1989). After experimenting with a several acids and etching times, a 40 second immersion in 10 % nitric acid solution was found to be appropriate to produce pore sizes in the desired range.

To etch only the shoulder bands of the implants, first masking tape was wrapped around the shoulder band, then the entire implant was dipped in melted paraffin wax and cooled. The masking tape was peeled off to leave the shoulder bands exposed, whereas the wax layer protected the remaining parts of the implant acted as a protection from the acid. After immersion in acid for the etching process, the implants were immediately rinsed in distilled water three to four times. The implants were then repeatedly swirled in xylene until the wax was completely removed. After ultrasonic cleaning, the etched implants were fired to 500°C to vaporize any residue.

Osteoceramic Characterization

In order to characterize the osteoceramic material, its crystal structure was determined using x-ray diffraction, and its surface structure was examined using a scanning electron microscope. Image analysis was applied to quantify the pore structures of each surface.

X-Ray diffraction

The raw materials used for the implants, calcium phosphate tribasic and magnesium aluminate spinel, have previously been identified in the raw material stage using

X-ray diffraction (Graves, 1988). She found that the calcium phosphate tribasic (Mallinkrodt, Inc.) was actually hydroxyapatite $[Ca_{10}(PO_4)_6(OH)_2]$ and that the magnesium aluminate spinel (Baikowski International Corporation) was fully converted spinel $[MgAl_2O_4]$.

To identify the sintered osteoceramic composite using x-ray diffraction and verify previous results found by Graves (1988), discs made with calcium phosphate tribasic, spinel, and binder/plasticizer solution were prepared as described earlier and fired to 1450°C using the same heating and cooling rates as described for the implants. The discs were coarsely broken using a hammer impact mill and crushed further using a Spex impact mill with steel faces and balls for 15 minutes. The powder was sieved to assure a particle size of smaller than 80 µm. X-Ray diffraction was run on a Siemens D-500 unit at 50 kv and 25 mA with CuKα radiation. Phases were identified using ASTM Powder Diffraction Data file and compared to the results found by Graves (1988).

Scanning electron microscopy

One tooth root implant of each surface structure was prepared for electron microscopy by sputter coating them using a Polaron E 5100 sputter coater with a 60/40 platinum- palladium target for 4 minutes. The three

implant microstructures were examined using a JEOL JSM 35
scanning electron microscope using 20 kv and 40 mA. In
addition, the specimen was tilted by 7 degrees, and another
micrograph was taken to obtain a stereo image.

Image analysis of surface structures

Image analysis was used to quantify and evaluate the
pore sizes of each surface structure. Negatives from
randomly positioned scanning electron micrographs were
enlarged, micropores were traced onto white paper and
colored in with black. This was done to eliminate the
numerous gray scales of the original micrographs,
especially from the etched specimens. Consequently, for
the rough specimen only the micropores were traced.
Macropores of this specimen were hand measured. Video
images were acquired and processed using a Kevex Delta IV
unit. The programs Automated Image Analysis and Feature
Analysis were used to analyze at least 163 features of each
surface structure. The feature analysis parameters used
were feature area, feature perimeter, breadth, height and
Waddel diameter. The Waddel diameter, also called the
nominal diameter, is defined as the diameter of a circle
having the same area as the feature. The breadth and
height are the ferret diameters in the x and y directions,
respectively, and are also called the tangent diameter of

the caliper diameter. The feature perimeter is the perimeter of the feature, just as the feature area is the area of the feature without holes. Statistical analysis and distribution curves of the parameters were compiled.

Implantation Procedure

Prior to implantation, all implants were measured to record shaft diameter, shoulder height and shoulder diameter. Then all the implants were sterilized in an autoclave. Anesthesia was induced using Surital® (17.5 mg/kg) intravenously to effect and maintained using 1-2% halothane gas. Atropine sulfate (0.5 mg/kg) was administered subcutaneously to the dogs which needed a cholinergic blocking agent to increase the pulse rate. Figure 9 is a schematic illustration showing the major implantation steps which are described as follows. For 9 of the 10 dogs a mucoperiosteal buccal-lingual flap extending over the 2nd, 3rd, and 4th premolar sites of the mandible was cut, and the soft tissue was elevated carefully from the osseous crest of the ridge and the buccal portion of the alveolar ridge. For the first dog in the implant study (8732), the pilot subject, two flaps were cut bilaterally to cover each implant individually. In all dogs two implants were placed on each side of the mandibles
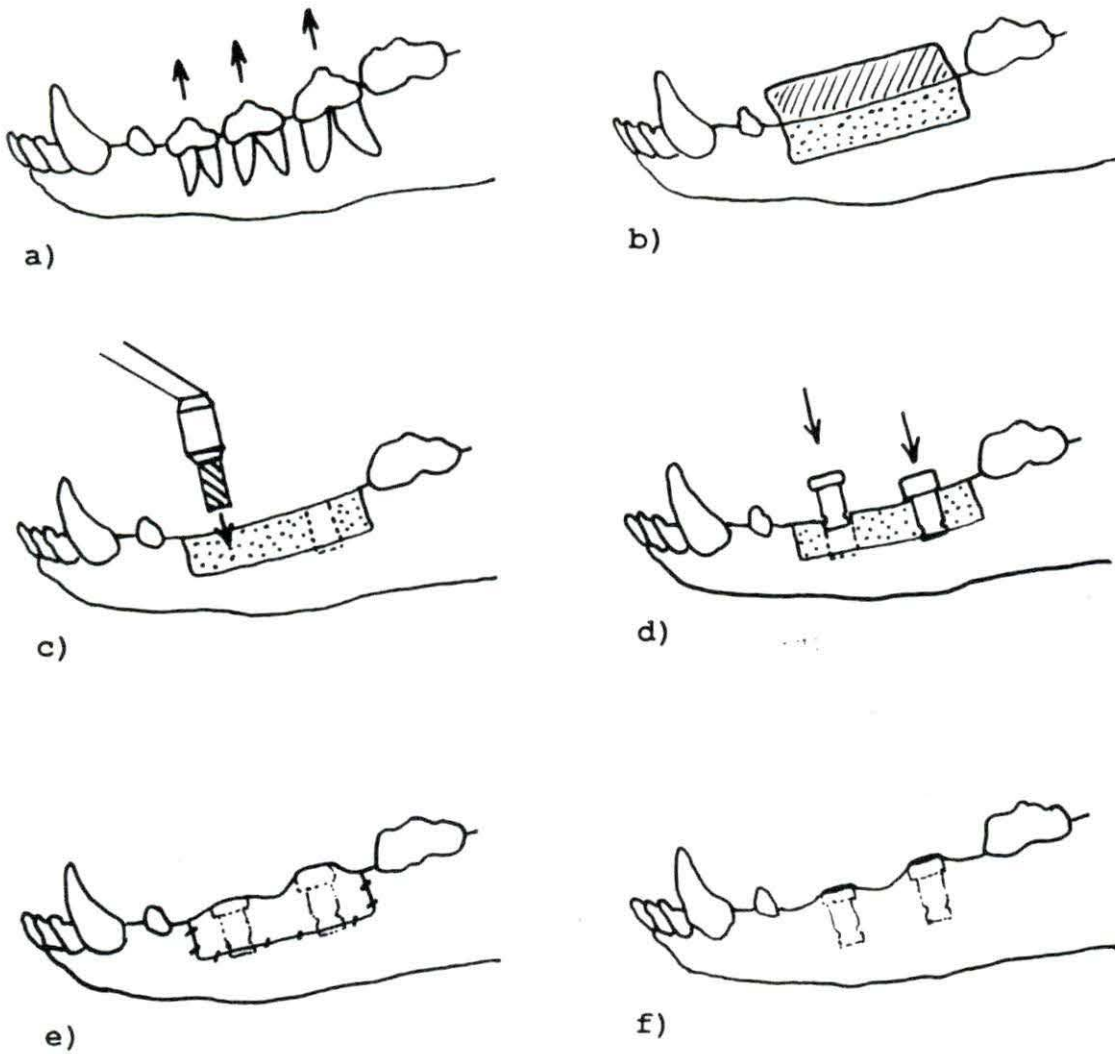
Figure 9.   Schematic illustration of the major
             implantation steps in the canine mandible. a)
             extraction of 2nd, 3rd, and 4th premolars, b)
             cutting of mucoperiosteal buccal-lingual flap,
             c) two holes drilled in alveolar bone, d)
             implants placed in drilled holes, e) flap
             placed back over implants and sutured, and f)
             healed tissue ready for gingiva cut-back

to assure ample space between the implants and to keep their responses from interfering with each other. A variable speed Skil® drill with maximum rpm of 350 was used to drill two holes in each side of the exposed alveolar mandibular bone. For each implant receptor site, a pilot hole was first drilled using a 2.5 mm drill bit. Then the hole was enlarged to 3.5 mm using minimum speed (250 rpm) with liberal application of topical saline to keep bone damage minimal. Excessive heating and surgical trauma can cause damage to the surrounding bone tissue and disturb the bone regeneration capacity of the vital bone tissue (Eriksson and Albrektsson, 1984). This process was repeated again using a 3.6 mm drill bit. In some cases, the 3.6 mm drilled hole was too small, so a 3.8 mm bit was used to enlarge the hole. For some of the later implant procedures (8736, 8724), the top of the ridge was filed off to flatten it. This provided more contact area between the shoulder and the alveolar ridge. Thirty-two implants were placed in 8 dogs. Two dogs (8724, 8736) had only 1 mm implants placed to document short-term bone response at 20 and 33 days. Implant distribution is shown in Table 6. The as fired surface with a slightly irregular surface structure was the control surface. Each dog had at least

Table 6. Implant distribution

Shoulder Height	Shoulder Surface	Total Nr.[a]	Short Term 20 d[b]	33 d	Post Cut-back 1 m[c]	3 m	6 m	12 m
1 mm	IR[d]	9	4	4	1			
2 mm	IR	6			1		2	3
	RO[e]	5			2	2		1
	SM[f]	4				2		2
2.6 mm[g]	IR	1					1	
3 mm	IR	5			1	2	1	1
	RO	5			2	1	2	
	SM	4			2	1	1	
4 mm	IR	1						1
Totals		40	4	4	8	8	8	8

[a]Total Nr. = total number of implants of a specific shoulder height and surface structure.

[b]d = length of implantation time in days.

[c]m = length of implantation time in month(s) following gingiva cut-back.

[d]IR = irregular surface.

[e]RO = rough surface.

[f]SM = smooth surface.

[g]2.6 mm = error in lathing process, unintentional shoulder height implanted in one dog.

one implant with this surface. Both the shoulder height
and the shoulder surfaces were varied. Consequently,
several dogs (8732, 8725) had varying shoulder heights with
control surfaces implanted while other dogs (8722, 8734)
had constant shoulder heights with varying shoulder
surfaces implanted. Specific details with regard to type
of implants and positions in each animal are shown in the
Appendix.

The implant fit snugly into the bone cavity allowing
the shoulder of the device to rest on top of the alveolar
ridge. The gingival flap was placed back over the implants
and sutured using 3.0 chromic gut[6]. At this point,
radiographs were taken to assess placement of implants and
to document bone gap area around the implant. Dogs were
given no food for 48 hours, then soft food only until the
gingiva was cut back. One dog (8725) was put on
amoxicillin for 14 days at 600mg/day because of local
infection of the surrounding tissue caused by the premature
protrusion of the 4mm implant through the gingiva.

---

[6]Ethicon, Inc., Somerville, NJ.

Examination Procedure

Clinical evaluation and gingiva cut-back

Following the implantation surgery, dogs were examined
every two weeks until the gingiva was cut back. The
clinical examinations before the gingiva cut-back consisted
of visual examinations of the implant sites, photographs of
the sites, and radiographs. The gingiva was cut back to
expose the implant between 4 and 8 weeks post
surgery. Even though some implants had already protruded
the gingiva prior to cut-back, they were completely cut
back at the designated cut-back date. Appendix 1 shows the
exact dates of cut-back for each dog. The short term dogs
(8724, 8739) did not have the gingiva cut back. For the
cut-back procedure, a scalpel was used to circularly cut
the gingiva off above the implant shoulder. After cut-
back, dogs were kept on soft food for at least 1 month.
Examinations after cut-back of gingiva were done at
approximately two weeks, one month, two, three, four, five,
six and nine months depending on the total implantation
time. The post cut-back examinations consisted of visual
examinations, probing, photographs and radiographs.
Numerical indexes were used to evaluate gingival bleeding,
mobility and plaque, and calculus (Koth et al., 1985) and
are shown in Table 7, 8, and 9, respectively. The

Table 7. Gingival bleeding index

Grade	Clinical Impression
0	Gingiva has normal color and stippling, no bleeding on probing
1	Gingiva has normal to slightly hyperemic color and stippling, no bleeding on probing
2	Gingiva hyperemic with redness and loss of stippling, bleeding on probing
3	Gingiva markedly red, edematous, spontaneous bleeding on finger pressure

Table 8. Mobility index

Grade	Clinical Impression
0	No mobility
1	Slight buccal-lingual mobility, < 0.5 mm
2	Slight buccal-lingual mobility, > 0.5 mm but < 1.0 mm
3	Mobility > 0.5 mm in buccal-lingual and mesial-distal directions
4	Depressible

Table 9. Plaque and calculus index

Grade	Clinical Impression
0	No plaque can be scraped off No calculus
1	Plaque can be scraped off but is not or only slightly visible to the clinician
2	Visible plaque on the tooth/implant and gingival margin; but plaque is not a heavy accumulation
3	Heavy accumulation of plaque on the tooth/implant and gingival margin

numerical evaluation was started about 3 months after some of the implants had already been cut back, therefore some of the initial indexes were not measured.

The left or right 1st mandibular molars were the control teeth. The entire clinical evaluations were performed by the same person. Some researchers (Koth et al., 1985) have stated that probing of the sulcus damages the seal which is forming between the gingiva and the implant, but the National Institute of Health (Schnitman and Shulman, 1980) feels that this measurement is absolutely necessary. Further, if the measurements are done, they should be taken from all four quadrants around the implant (Schnitman and Shulman, 1980). Because of our design with the shoulder portion extending over the

bone/implant interface, probing of sulcus depth actually only measures gingiva height. To probe the sulcus, a calibrated dental probe was used to measure the control tooth and four locations around the implant: mesial, buccal, distal and lingual.

The process to determine the gingival bleeding index started with visual inspection, then digital pressure was applied, followed by probing of the gingival sulcus. To determine the mobility indexes, a blunt instrument was placed against the implant and then pushed in different directions. Depression and rotation was rated by applying finger pressure in different directions.

Radiographic evaluations

Radiographs were examined to observe bone response to the implant. Two evaluation methods were used. The first was to apply the numerical indexes shown in Table 10 (McKinney et al., 1982) to evaluate the bone resorption around the implants. The second method was to measure the alveolar ridge height adjacent to the implant. Because there was no specific radiographic set-up to reproduce radiographs at the same angle every time, the measurements had to be standardized. This process was done by measuring the total height of the implant, the height of the bone

Table 10. Radiographic index

Index	Radiographic parameter
0	No radiographic evidence of bone resorption around the implant
1	Slight (less than 0.5 mm) resorption of alveolar bone around the implant
2	Moderate (0.5 mm - 2mm) resorption of alveolar bone around the implant
3	Severe (more than 2mm) resorption of alveolar bone around the implant
4	Radicular radiolucency greater than 1.5 mm wide and along more than 1/3 of the root surface

ridge directly adjacent to the implant on both the mesial and distal sides, taking the ratio of the two and multiplying by 100 to obtain a percentage. This percentage gives the relative vertical height of the alveolar ridge adjacent to the implant. In order to assess a comparable change in alveolar ridge height, differences between consecutive readings were calculated to obtain a trend.

Bone Labeling

Fluorescence labeling is a technique with which the location and time of bone regeneration can be identified.

Tetracyclines and dyes are two types of fluorochromes used to label bone. By using sequential fluorochromes with different excitation and emission wavelengths, clearly contrasting colors can illustrate the ossification process. These colors will be displayed by the histological sections when viewed using a fluorescence microscope.

For this study four fluorochromes were administered before the animals were euthanized: demeclocycline, oxytetracycline, xylenol orange, and alizarin Red S. Alizarin red S[7] (35 mg/kg) was administered intravenously to only one dog as a 1 % aqueous solution. This fluorochrome produces red fluorescence. Harris et al. (1964) stated that acute toxic symptoms were rare at dose levels under 40 mg/kg, yet the dog in this study injected with a 35 mg/kg dose had nausea, vomiting, weakness, and muscular rigidity, which are the symptoms due to toxicity from the alizarin red S. After 4 days, the dog's symptoms were not improving and the dog was therefore euthanized 4 days earlier than scheduled. Due to the adverse affects of this bone labeling substance, it is not recommended for such use. Demeclocycline[8] was given at 300 mg every 8

---

[7]Sigma Chemical Co., St. Louis, MO.

[8]Lederle Laboratories, American Cyanamid Comp.

hours for 3 days to give a total dose of 2700 mg. Oxytetracycline[9] was given at 250 mg every 8 hours for 3 days to give a total dose of 2250 mg. Xylenol orange[10], a tetrasodium salt, was administered intravenously as a 3% aqueous solution at a dose of 90 mg/kg and a rate of 10 ml/min. Demeclocyline produces a green fluorescent band, oxytetracycline a light yellow fluorescent band, and xylenol orange an orange fluorescence. The dates of bone labeling for each time period varied and are listed in Appendix 1.

Euthanasia

Eight of the ten dogs were euthanized at the following times: one each at 20 days, 30 days after implantation; and two each at 1 month, 3 months, and 6 months after gingiva cut-back. The two remaining dogs have not been euthanized and will have a total time period of 12 months following gingiva cut-back. The dogs were euthanized with a 1 ml/10 lb dose of Beuthanasia-D[11] special euthanasia solution. The mandibles of the dogs were sectioned into

---

[9]Rugby Laboratories, Inc., Rockville Centre, NY.

[10]Sigma Chemical Co., St. Louis, MO.

[11]Schering Corporation, Kenilworth, NJ.

blocks containing an implant and fixed in 70% ethanol. Radiographs of the implant/tissue block were taken to obtain both lingual-buccal views and mesial-distal views. In future work, histological sections will be examined under a light microscope to study the cellular response of the tissues.

RESULTS AND DISCUSSION

The results will be presented in the following order: osteoceramic characterization, implantation observations, clinical and design evaluation.

Osteoceramic Characterization

<u>Crystallographic structure</u>

Analysis by X-ray diffraction of the osteoceramic composite fired to 1450°C confirmed that the two phases present were α-Ca$_3$(PO$_4$)$_2$ and MgAl$_2$O$_4$. Figure 10 shows the diffraction pattern for the osteoceramic with the peaks identified for each phase. When compared with the results found by Graves (1988), the diffraction peak angles were identical, therefore the two materials were crystallographically the same.

<u>Microstructure</u>

<u>Smooth</u>   Micrographs of the polished osteoceramic composite were taken at 1000 and 5000 magnification and are shown in Figures 11a and b, respectively. The surface is leveled with micropores distributed evenly. The micropores occur either from existing surface pores or from interior pores of the composite, which were exposed during polishing. Shallow depressions on the surface could be due
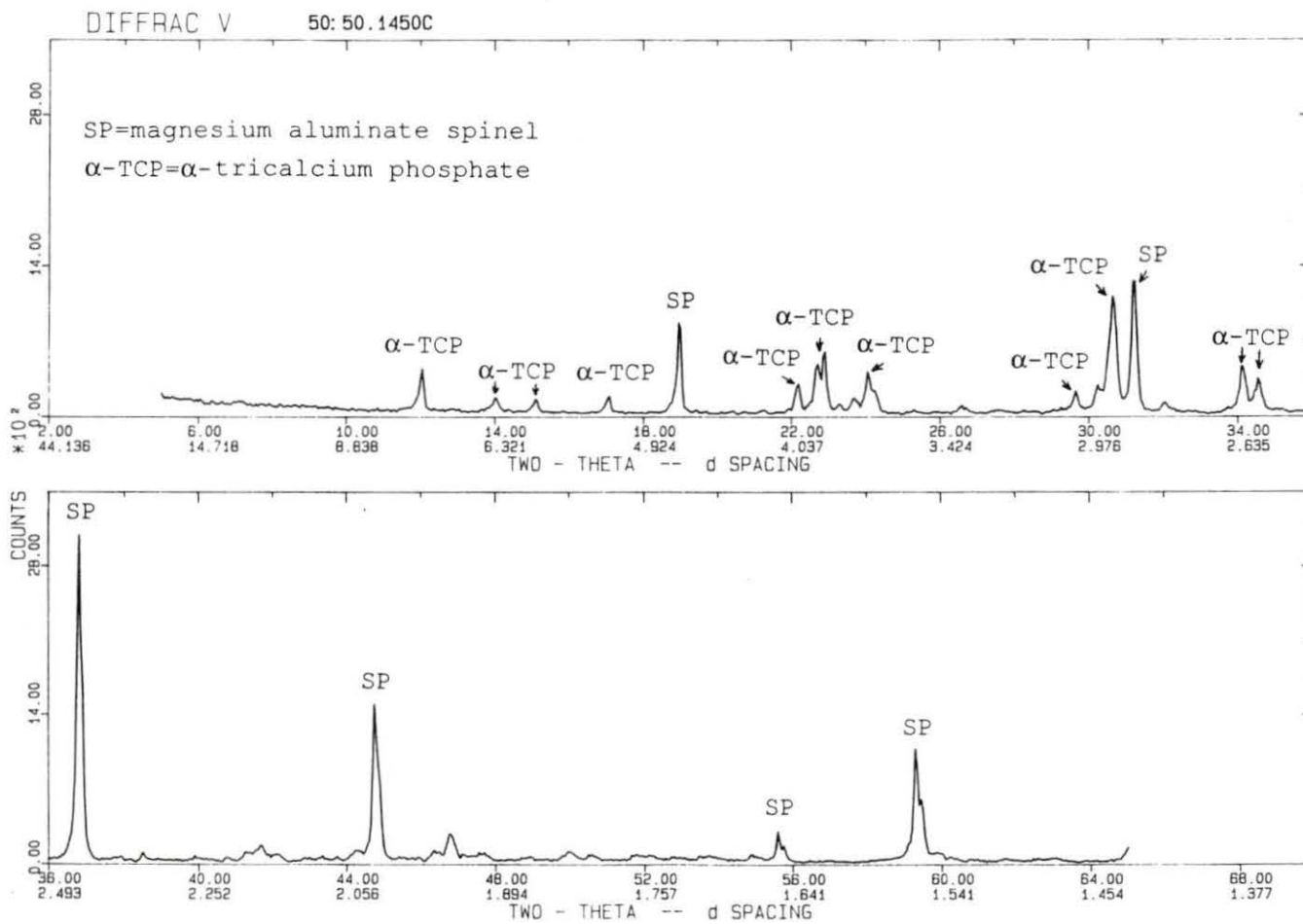
Figure 10. X-ray diffraction pattern of the osteoceramic material with the peaks identified

Figure 11.   Scanning electron micrograph of the smooth
              osteoceramic surface. a) 2,500x (bar=5 µm),
              b) 12,500x (bar=1 µm)
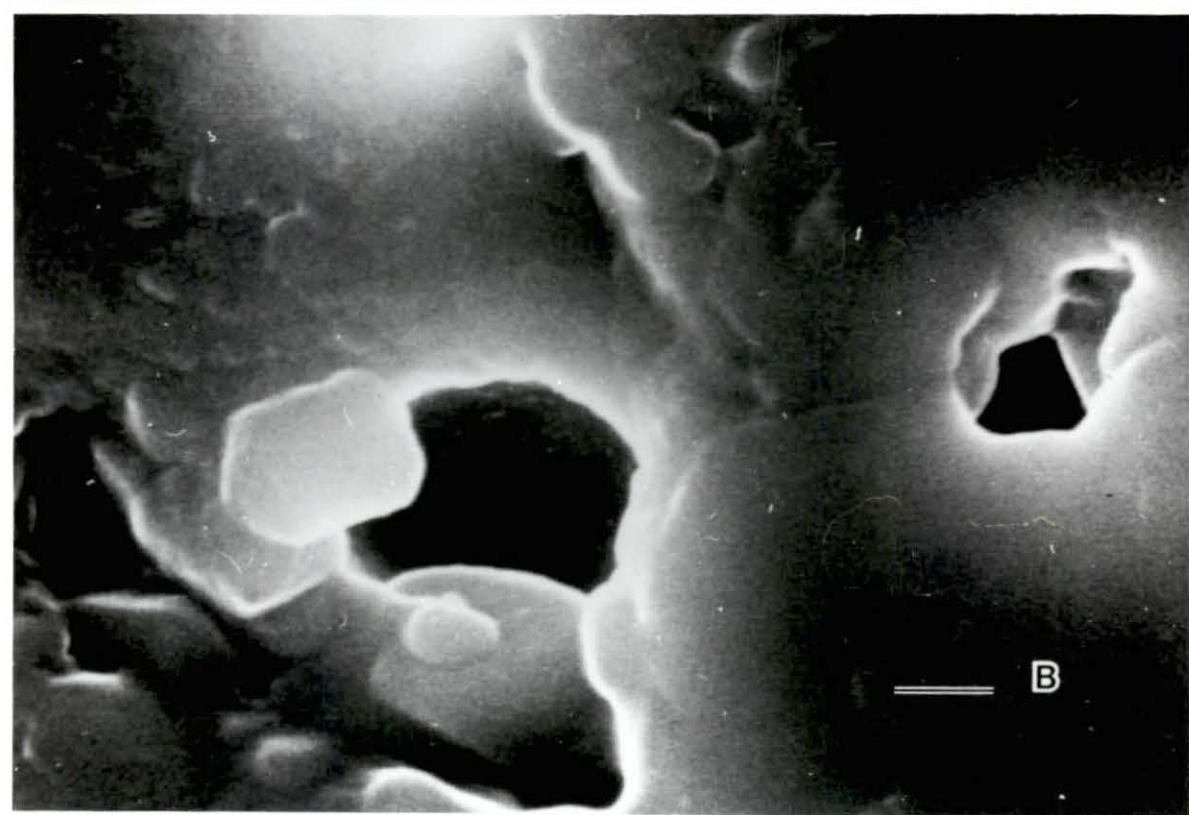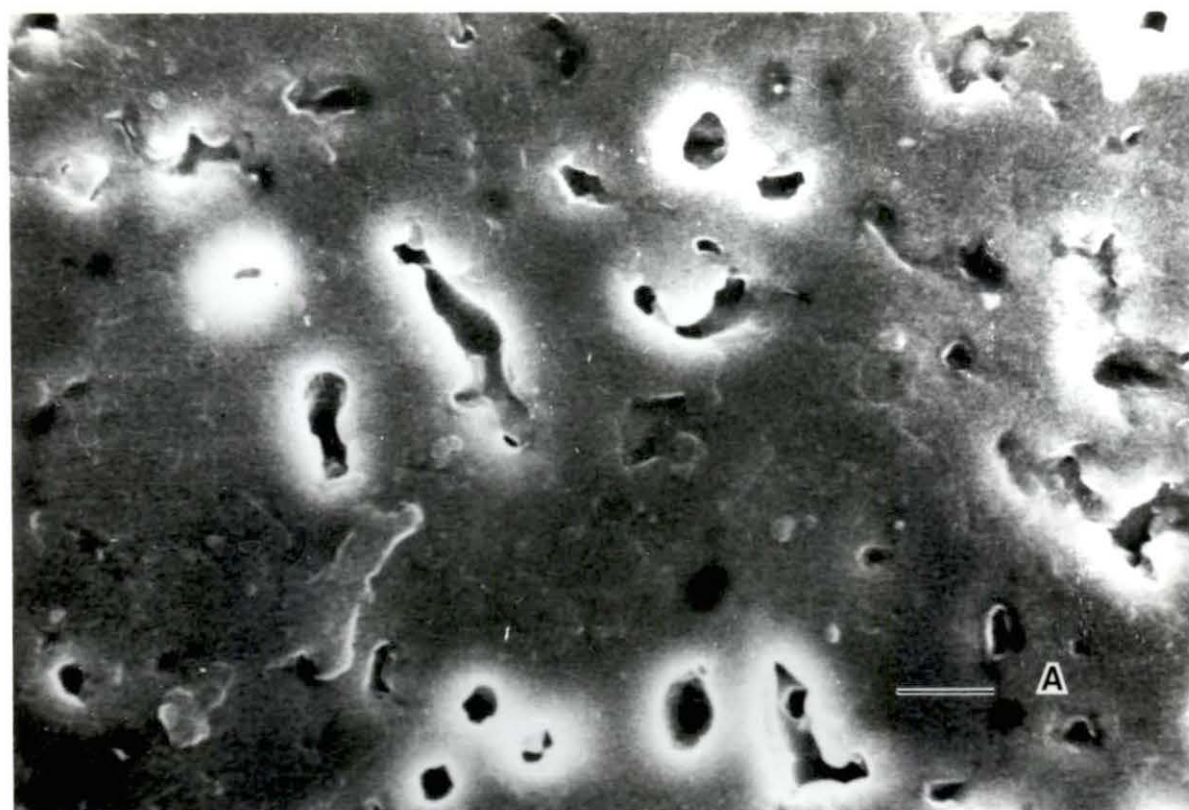
to tear-out of the soft calcium phosphate tribasic phase during the polishing process. When viewed with a stereoviewer, the stereo image in Figure 12 confirms the description of the smooth surface in a three dimensional aspect.

Irregular   Micrographs of the fired osteoceramic composite are shown in Figure 13a and b. In general, the surface has a melted-over appearance. Although the grains of material appear attached to one another, some cracking between grains is visible, especially in Figure 13b. This phenomena may be due to the cooling of the composite. Few pores are seen on the surface. The surface is slightly irregular with regard to surface undulations, which is displayed in the stereo image of Figure 14.

Rough   The etched surface of the osteoceramic composite is shown in the micrographs of Figure 15a and b. In the etching process, the softer phase, calcium phosphate tribasic, is removed leaving the surface with macropores and micropores. In Figure 15a, the macropores seen range from 9 to 17 μm in diameter, whereas the smaller pores range from 0.3 to 8 μm. Figure 15b, a close-up of the etched surface, shows the cubic crystal shape of the spinel with the calcium phosphate tribasic as a filler deeper within. Because the micropores are hard to see in a two-

Figure 12.   Stereo micrograph of the smooth osteoceramic
              surface at 2,500x (bar=5 μm)
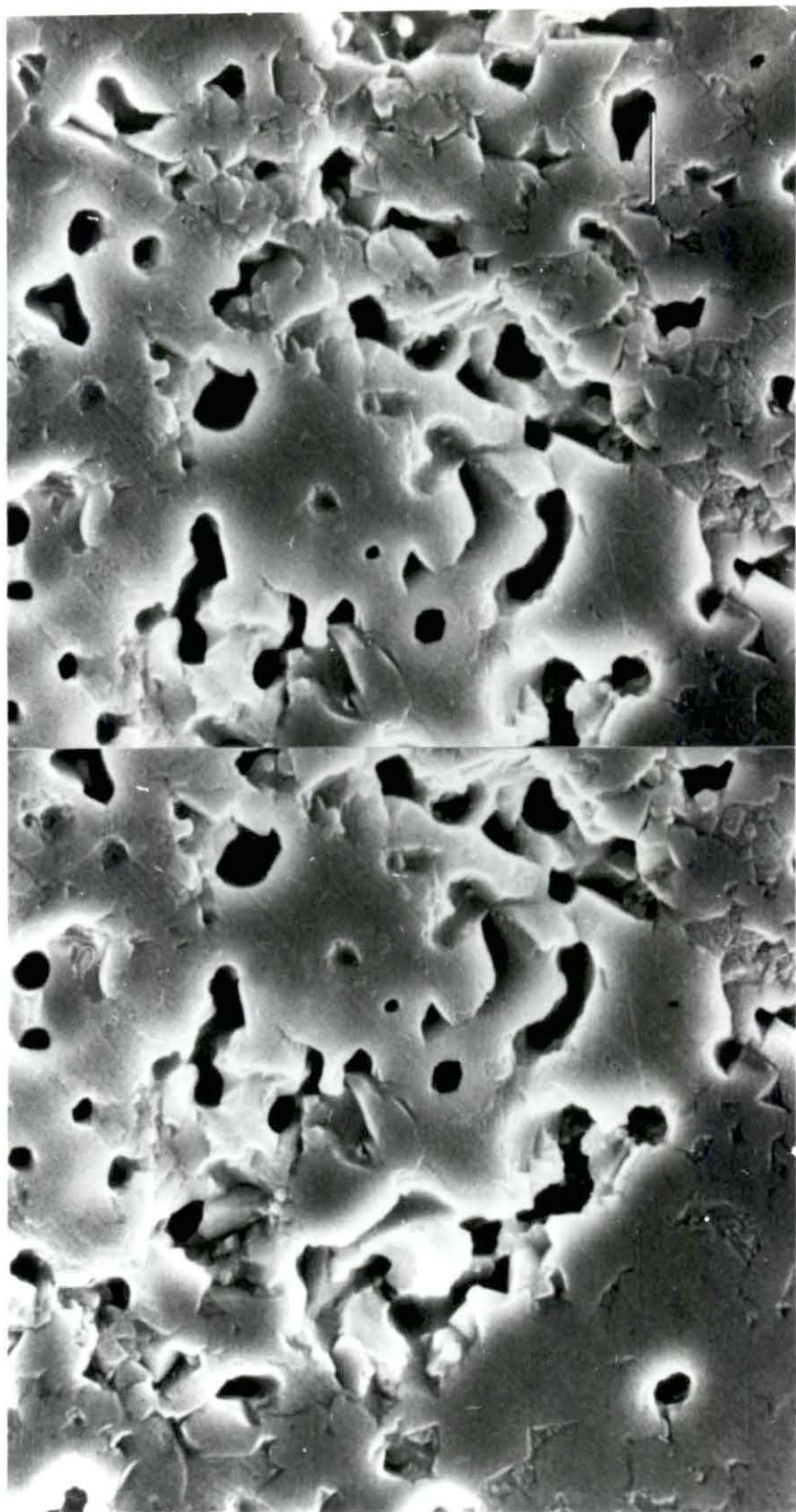
Figure 13.   Scanning electron micrograph of the irregular
              osteoceramic surface.   a) 2,500x (bar=5 μm),
              b) 12,500x (bar=1 μm)
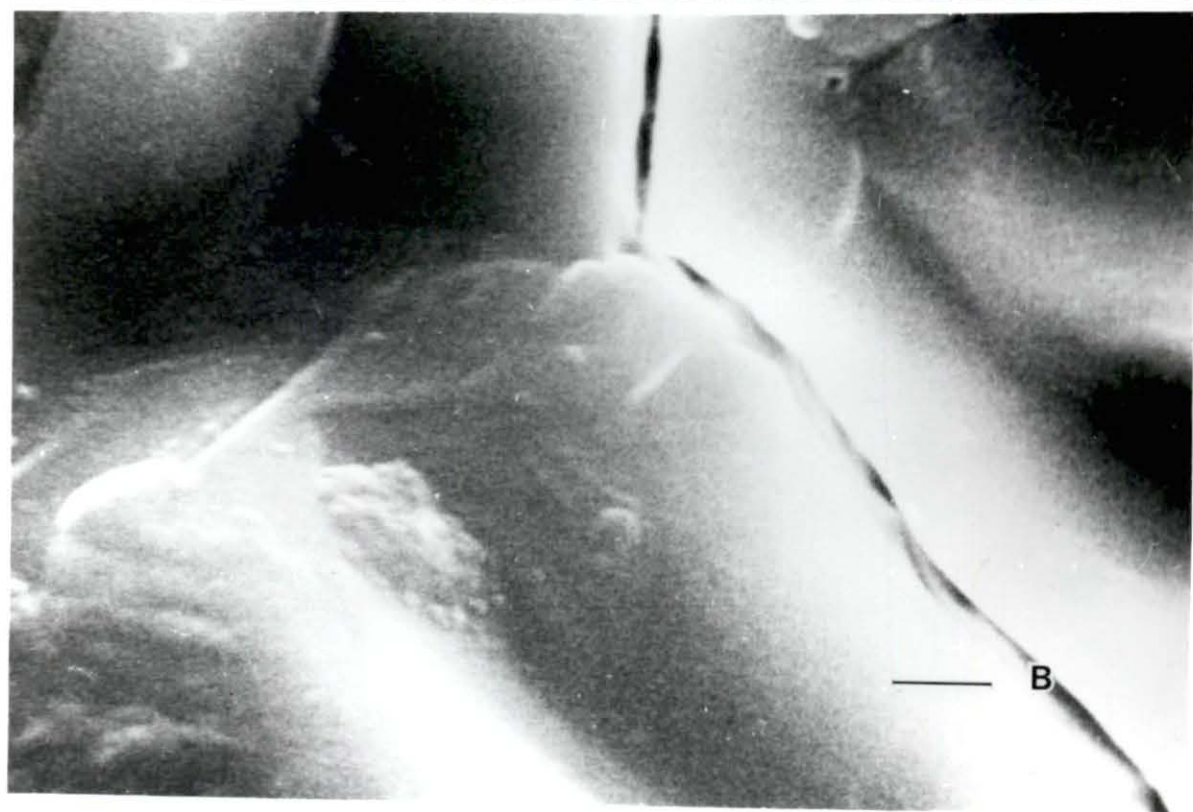
Figure 14.   Stereo micrograph of the irregular
              osteoceramic surface at 2,500x (bar=5 μm)
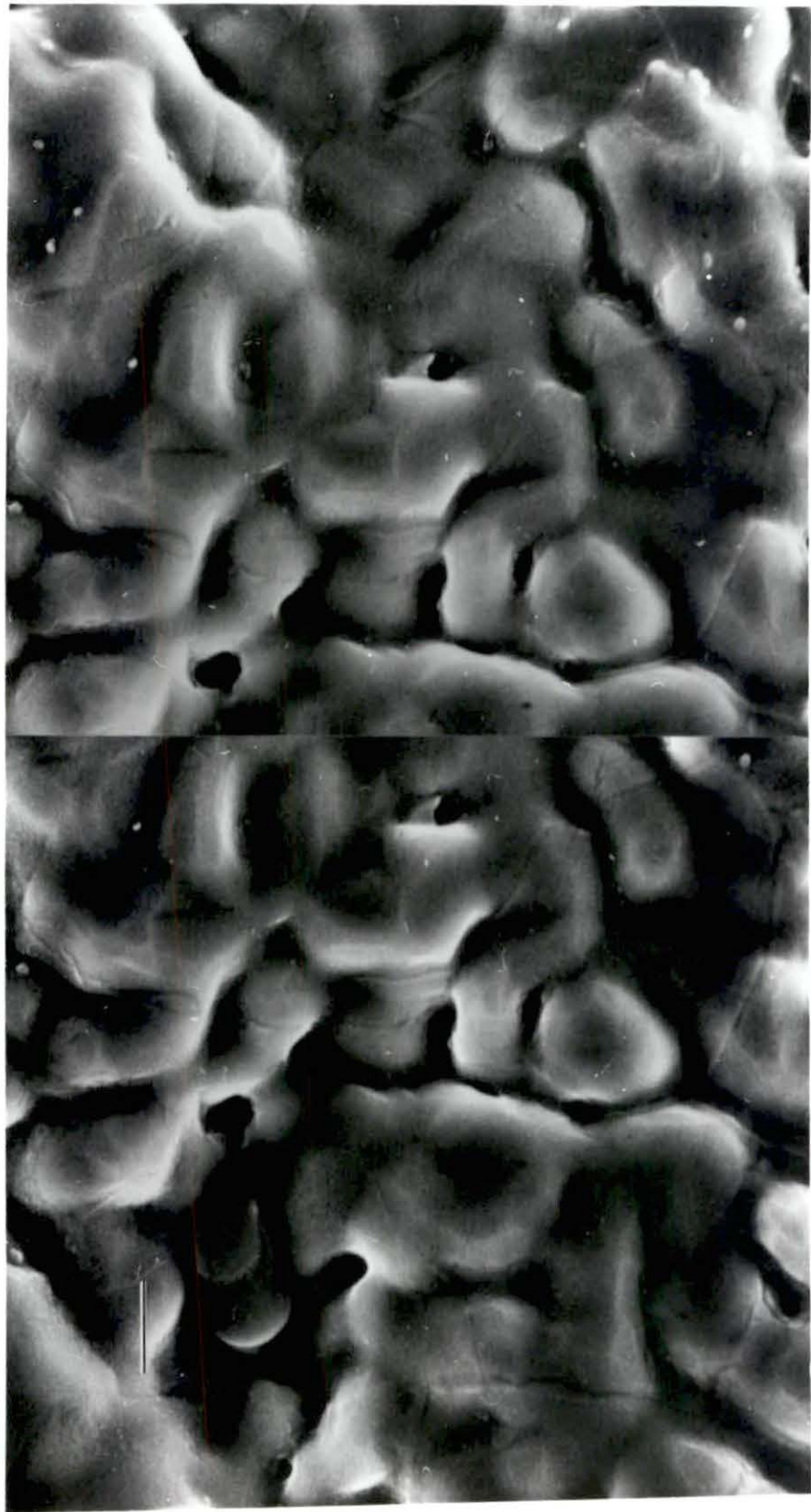
Figure 15.   Scanning electron micrograph of the rough
              osteoceramic surface.   a) 2,500x (bar=5 µm),
              b) 12,500x (bar=1 µm)
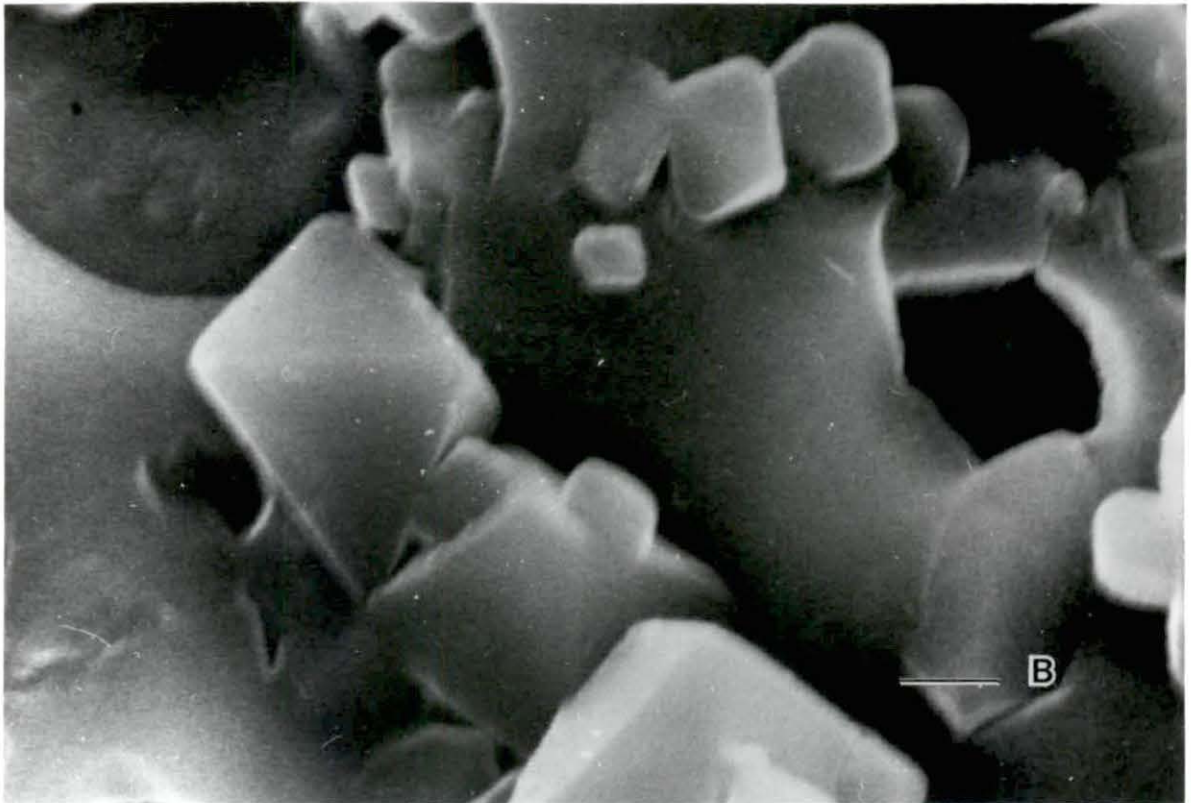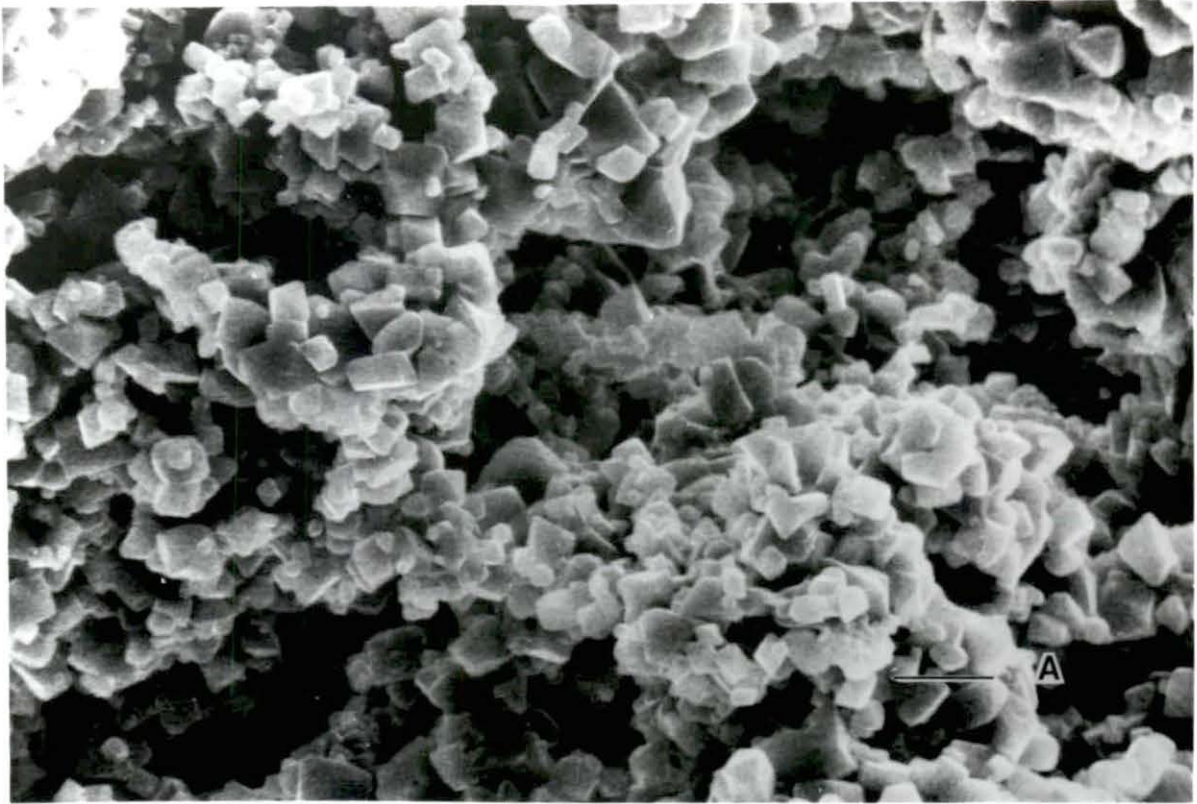
dimensional photo, the stereo image shown in Figure 16 gives a better representation of the complexity of this surface.

Pore Size Distribution

Smooth   Five micrographs from polished samples with a total of 186 features were analyzed. Table 11 gives the data which were found.

Table 11. Pore size data for the smooth osteoceramic

	Area	Perimeter	Breadth	Height	Wad Diam[a]
		(microns)			
Number	186	186	186	186	186
Minimum	0.12	0.88	0.47	0.08	0.39
Maximum	16.27	29.12	6.51	8.54	4.55
Average	3.06	7.11	2.32	1.80	1.79
St. Dev.	2.72	4.44	1.23	1.07	0.83
Sum	570	1323	432	335	333

[a]Wad Diam = Waddel diameter of the feature.

Taking the sum of all feature areas and dividing it by the total area of all the micrographs analyzed gives the percentage of surface area covered by pores. For the polished osteoceramic this calculated to be 7.34%.

Figure 16.   Stereo micrograph of the rough osteoceramic
              surface at 2,500x (bar=5 μm)
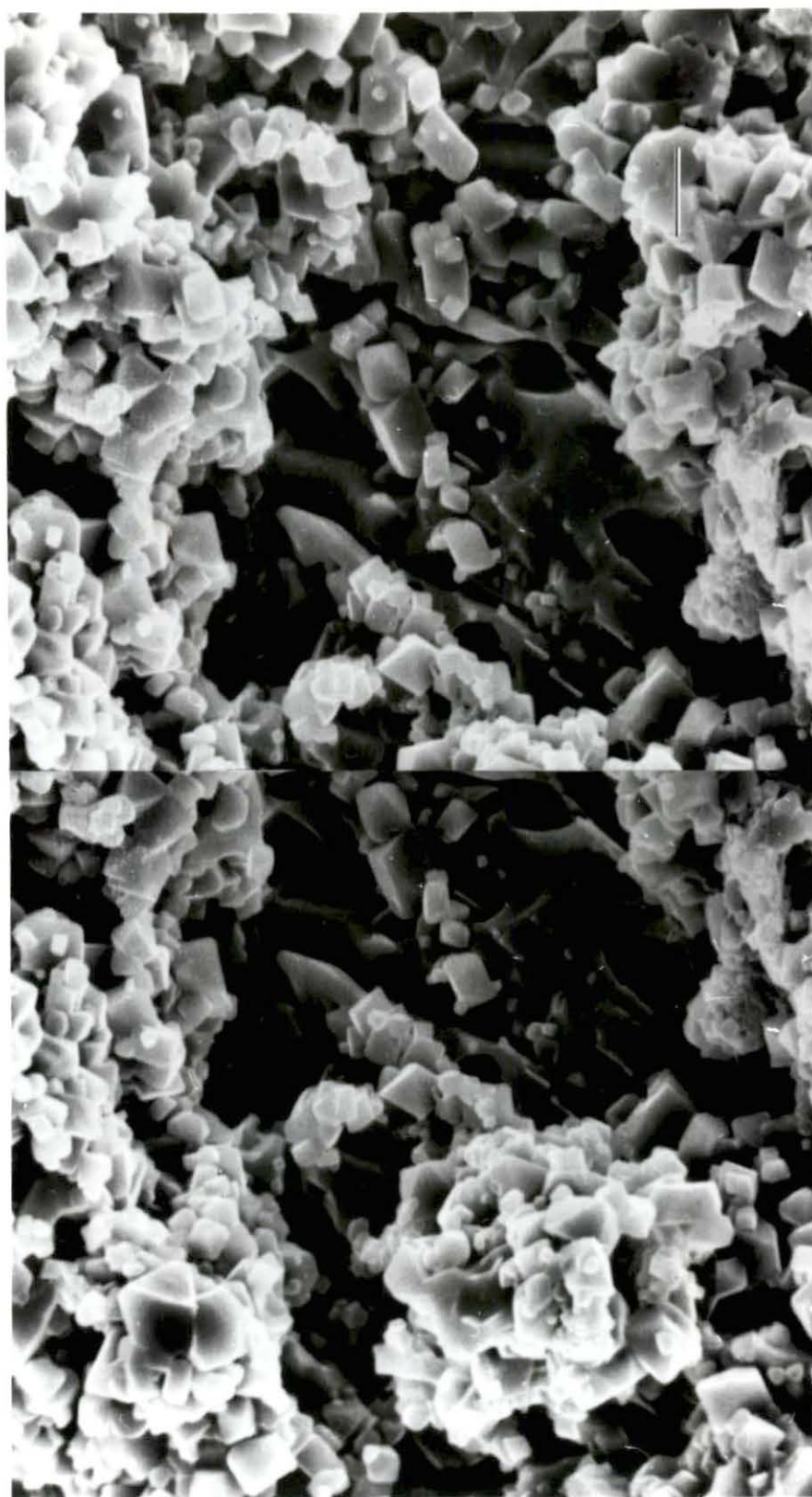
Because of the variety in pore shapes, the Waddel diameter was used to determine the diameter of a circular pore of equal area as the feature being analyzed. The Waddel diameter distribution for the polished surface is plotted over the applicable size range in Figure 17. The average Waddel diameter is 1.79 µm. From that histogram it can be seen that 47% of the pores fall into the 1.5 to 2.5 µm size.
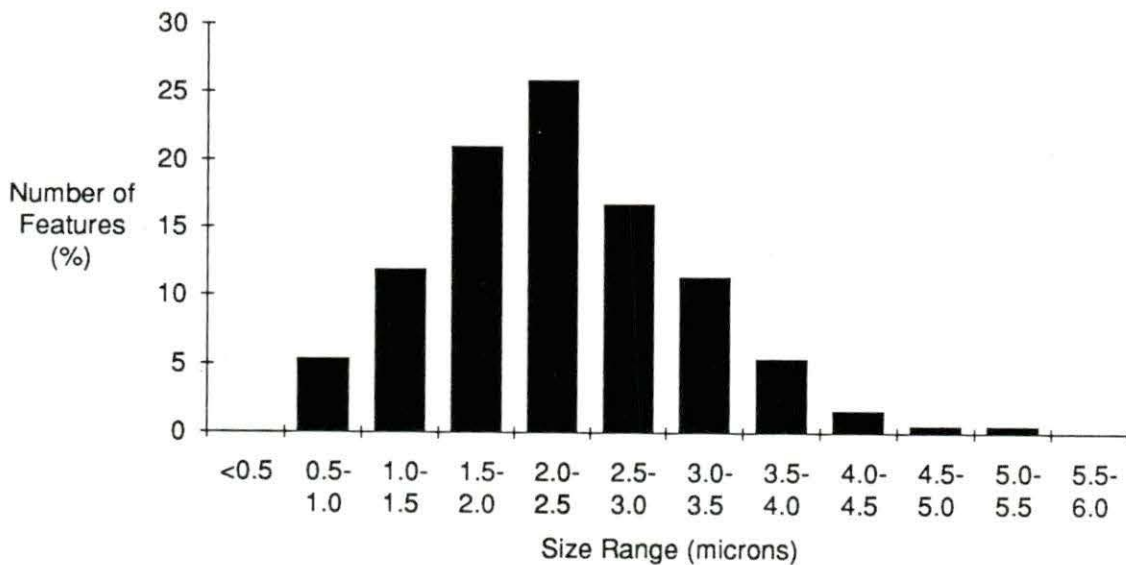
Figure 17. Histogram of the Waddel diameter distribution of the smooth osteoceramic

Irregular

For the as fired osteoceramic composite, five micrographs with 163 features were analyzed. Table 12 gives the data found.

Table 12. Pore size data for the irregular osteoceramic

	Area	Perimeter	Breadth (microns)	Height	Wad Diam[a]
Number	163	163	163	163	163
Minimum	0.13	1.81	0.73	0.69	0.80
Maximum	16.09	56.64	14.58	11.00	9.05
Average	1.32	8.76	3.10	2.23	2.35
St. Dev.	1.75	6.94	1.67	1.53	1.11
Sum	216	1428	505	364	383

[a]Wad Diam = Waddel diameter of the feature.

Only 0.69% of the surface area of the as fired composite is covered by pores. The Waddel diameter distribution is shown in Figure 18, where the average Waddel diameter is 2.35 μm. In the histogram, 51% of the pores fall into the 2.0 to 3.0 μm range.
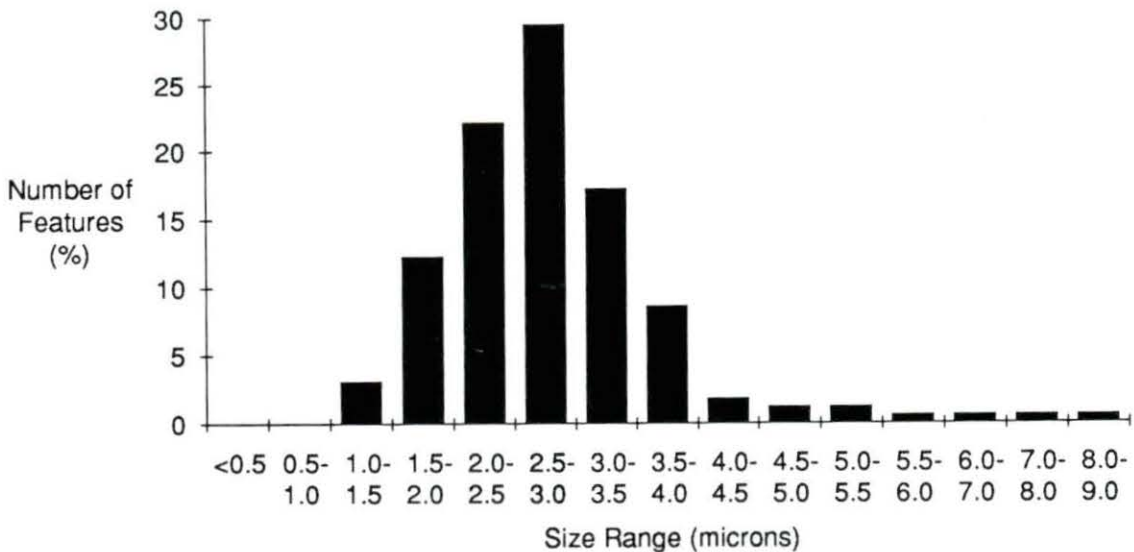
Figure 18. Histogram of the Waddel diameter distribution
of the irregular osteoceramic

Rough

Two micrographs with a total 384 features were
analyzed. Because of the extensive range of gray scales in
these micrographs only the pores colored black were
considered for the image analysis. The data for these
pores, which are the micropores of the surface, are given
in Table 13. The data from the macropores of this surface
were not calculated using the image analysis program but
rather hand measured. The macropores were measured to be
between 8 and 17.5 μm in diameter, with an average diameter

Table 13. Pore size data for the rough osteoceramic
           (micropores only)

	Area	Perimeter	Breadth	Height	Wad Diam[a]
			(microns)		
Number	384	384	384	384	384
Minimum	0.13	0.68	0.73	0.34	0.80
Maximum	11.60	59.92	16.77	8.94	7.68
Average	1.05	8.12	2.88	1.93	2.01
St. Dev.	1.36	7.42	2.05	1.28	1.14
Sum	404	3116	1105	739	771

[a]Wad Diam = Waddel diameter of the feature.

of 13.8 µm ± 4.35 µm. Taking both the micropore and
macropore measurements into account, the percentage of
surface area covered by pores was calculated to be 14.1%.

The Waddel diameter distribution for only the
micropores is shown in Figure 19. Of the micropores, 62%
fall into the 1.0 to 2.5 µm range.

Implantation Observations

The implantation procedure using a mucoperiosteal
buccal-lingual flap functioned well. Through the
experience of several surgeries, it was observed that a
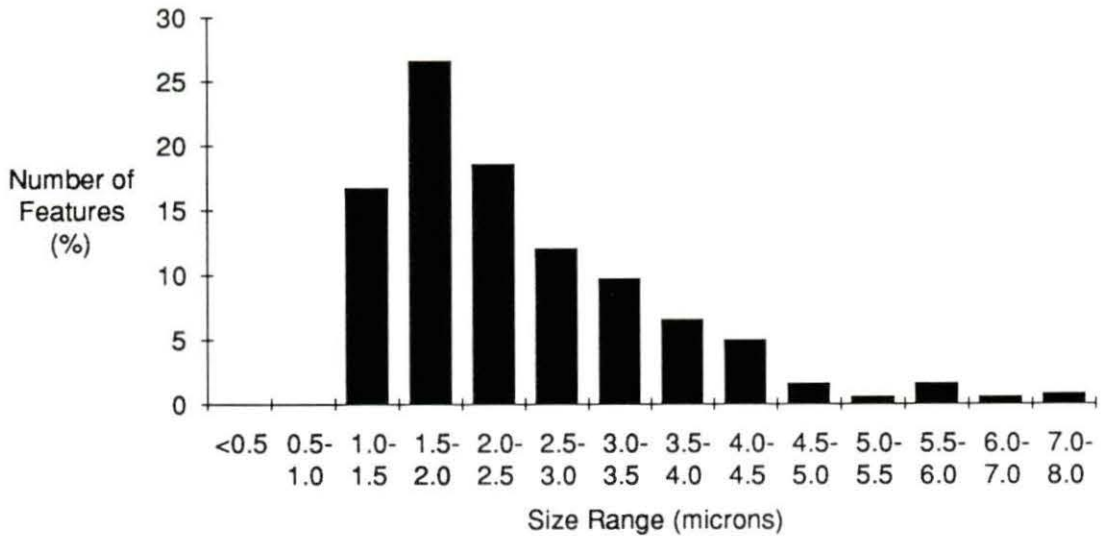
Figure 19. Histogram of the Waddel diameter distribution of the rough osteoceramic

sharp alveolar ridge did not allow maximum contact between the lower surface of the shoulder and the top of the ridge. Consequently, this gap might cause an inclusion where bacteria and debris could start an infection. For two short term dogs (8734,8724), the crest of the alveolar ridge was filed flat to permit the shoulder to sit flat on the alveolar ridge and allow more contact between the shoulder and the underlying bone.

The position of the suture line had an effect on the implant staying covered by the gingiva for the entire healing period. For several surgeries, the suture line was positioned exactly at the edge of the implant shoulder which may have led to premature cut through of the implant. In the following surgeries, the suture line was cut more buccally to alleviate this problem.

In drilling the holes for the implant, consideration was given to placing them vertically in the alveolus. In later examinations and in the tissue/implant block radiographs, the observation was made that some implants angled buccally. This probably put more pressure on the buccal portion of the alveolus. Another consequence of this is that the contact area of the underlying alveolar bone with the shoulder is less buccally than lingually.

Clinical Evaluations

The clinical evaluations of the control teeth at 8 time periods are listed in Table 14. The results of the clinical evaluations of the smooth, irregular, and rough surfaced implants at 8 time periods are listed in Tables 15, 16, and 17, respectively. The tables give the number of data points in the samples, the means and standard

Table 14. Clinical evaluation of the control teeth

	Time Period							
	2 wks	1 mo	2 mo	3 mo	4 mo	5 mo	6 mo	9 mo
Bleeding Index	3[a]	1	3	1	3	2	2	2
	1.67[b]	3.00	3.00	0.50	1.67	2.50	2.00	1.50
	(1.53)	(-)	(0)	(-)	(1.53)	(0.71)	(1.41)	(0.71)
Mobility Index	3	2	2	2	3	2	2	2
	0	0	0	0	0	0	0	0
Plaque Index	3	2	2	2	3	2	2	2
	2.00	2.00	2.50	2.25	1.29	2.50	2.00	1.50
	(0)	(0)	(0.71)	(0.35)	(0.51)	(0.71)	(0)	(0.71)
Sulcus Depth (mm)	3	1	2	-	3	2	2	2
	2.89	2.64	1.70	-	2.17	1.94	2.15	2.03
	(1.73)	(-)	(0.78)	-	(0.41)	(0.11)	(0.15)	(0.02)

[a]Sample number.

[b]Mean (standard deviation).

94

Table 15. Clinical evaluation of the smooth osteoceramic implant

| | Time Period | | | | | | | |
	2 wks	1 mo	2 mo	3 mo	4 mo	5 mo	6 mo	9 mo
Bleeding Index	5[a] 2.30[b] (0.84)	3 1.68 (0.59)	3 2.63 (0.65)	3 0.50 (0.50)	3 2.67 (0.58)	1 2.00 (-)	2 2.00 (0)	1 2.50 (-)
Mobility Index	5 0	3 0	3 0	3 0	3 0	1 0	2 0	1 0
Plaque Index	5 1.50 (0.71)	3 1.33 (0.58)	3 1.34 (0.48)	3 1.00 (1)	3 1.63 (0.55)	1 2.50 (-)	2 2.00 (1.41)	1 2.50 (-)
Sulcus Depth (mm)	4 3.10 (1.32)	2 2.63 (1.06)	3 4.00 (1.60)	- - -	3 3.63 (0.39)	1 3.41 (-)	2 3.15 (1.12)	1 4.31 (-)
Radiograph Index	8 .75 (0.89)	5 .80 (0.84)	6 1.00 (0.89)	6 1.00 (0.89)	3 1.00 (1.00)	1 1.00 (-)	3 1.33 (0.58)	2 1.50 (0.71)
Ridge Loss (%)	8 -2.25 (5.06)	5 2.00 (13.30)	6 2.00 (8.99)	6 -2.33 (6.68)	3 -0.67 (2.52)	1 4.00 (-)	3 -4.00 (7.55)	2 2.00 (7.07)

[a]Sample number.

[b]Mean (standard deviation).

Table 16. Clinical evaluation of the irregular osteoceramic implant

	2 wks	1 mo	2 mo	3 mo	4 mo	5 mo	6 mo	9 mo
				Time Period				
Bleeding Index	4[a] 2.25[b] (0.50)	2 1.50 (0.71)	2 1.94 (0.08)	8 1.38 (0.52)	4 2.75 (0.50)	3 2.67 (0.58)	5 2.96 (0.09)	4 2.75 (0.50)
Mobility Index	4 0	2 0	2 0	8 0	4 0	3 0	5 0	4 0
Plaque Index	4 1.25 (0.50)	2 2.00 (0)	2 1.44 (0.62)	8 1.63 (0.74)	4 1.50 (0.58)	3 1.50 (0.71)	5 3.00 (0.71)	4 3.00 (1.15)
Sulcus Depth (mm)	3 3.47 (0.90)	1 1.5 (0)	2 1.97 (0.66)	– – –	4 3.21 (1.12)	3 2.81 (0.88)	5 3.91 (0.65)	4 3.56 (0.66)
Radiograph Index	14 0.64 (0.63)	4 0.50 (0.58)	12 0.75 (0.75)	12 0.67 (0.65)	6 0.83 (0.75)	5 0.40 (0.55)	10 0.60 (0.70)	5 0.80 (0.84)
Ridge Loss (%)	14 -2.0 (3.82)	4 2.75 (8.62)	12 -0.67 (5.12)	12 -2.42 (3.60)	6 1.5 (0.84)	5 -1.8 (2.77)	10 -1.6 (5.25)	5 -4.8 (6.06)

[a]Sample number.

[b]Mean (standard deviation).

Table 17. Clinical evaluation of the rough osteoceramic implant

	Time Period							
	2 wks	1 mo	2 mo	3 mo	4 mo	5 mo	6 mo	9 mo
Bleeding Index	7[a] 2.57[b] (0.53)	3 1.71 (0.62)	3 3.00 (0)	3 2.00 (1)	3 2.67 (0.58)	1 2.00 (-)	2 2.00 (0)	1 2.50 (-)
Mobility Index	7 .14 (.38)	3 0	3 0	3 0	3 0	2 0	1 0 (-)	1 0 (-)
Plaque Index	7 1.57 (0.78)	3 1.33 (0.58)	3 1.75 (0.54)	3 2 (1.00)	3 2.29 (0.51)	2 3 (0)	1 3 (-)	1 3 (-)
Sulcus Depth (mm)	4 3.26 (1.42)	1 4.31 (-)	3 3.63 (0.88)	- - -	3 3.72 (1.31)	2 3.96 (0.77)	1 2.63 (-)	1 3.56 (-)
Radiograph Index	10 0.50 (0.71)	7 1.14 (0.90)	6 0.67 (0.82)	6 0.67 (0.82)	3 0.33 (0.58)	2 0.50 (0.71)	3 0.67 (0.58)	1 0 (-)
Ridge Loss (%)	10 -2.10 (4.36)	7 -0.30 (4.80)	6 0.50 (7.23)	6 0.17 (5.91)	3 -0.67 (3.79)	2 -2.00 (1.41)	3 1.67 (13.00)	1 -2.00 (-)

[a]Sample number.

[b]Mean (standard deviation).

deviations for the gingival bleeding index, mobility index, plaque and calculus index, sulcus depths, radiographic index and vertical alveolar bone ridge loss.

Clinical results

From the visual observations during the clinical examinations, the following results regarding shoulder heights were found. A 1 mm shoulder was too low, because the gingiva grew back over 2 weeks after it was cut back. This is undesirable since bacteria and debris enclosed underneath the gingiva can lead to infection. Figure 20a shows the clinical response to a 1 mm shoulder which had allowed the gingiva to grow back over and become inflamed. Of the 2 mm implants, six shoulders had partially cut through at four weeks after implantation, and nine remained completely covered until to the cut-back procedure. Of the 2 mm implants only one had tissue grow back over. The causes for the partial cut through for the 2 mm implants can be attributed to one or more these influences: position of suture line directly at the edge of shoulder, degree of roundness of shoulder and tendency of the dog to chew on hard objects such as a metal cage. Of the 3 mm implants, 10 cut partially through the tissue prior to gingival cut-back leaving only four which remained

Figure 20.   Clinical reponse to the osteoceramic implant.
              a) dog 8732 at 2 months after gingiva cut-
              back with arrow showing a 1 mm implant
              covered by gingiva, b) dog 8725 at 2 weeks
              after implantation with arrow showing a 4 mm
              implant which has protruded the gingiva, c)
              dog 8734 at 6 months after the gingiva cut-
              back showing 2 mm implants with irregular
              (IR) and smooth (SM) surfaces
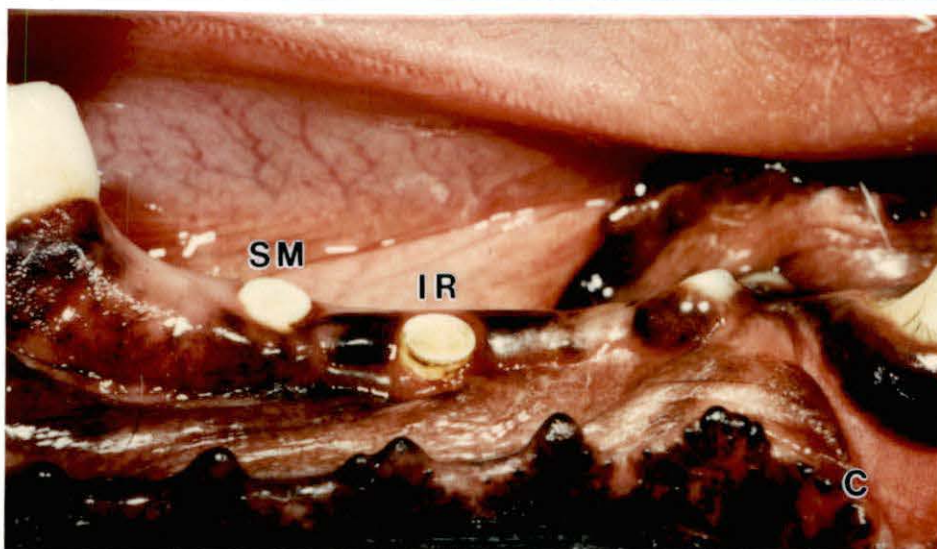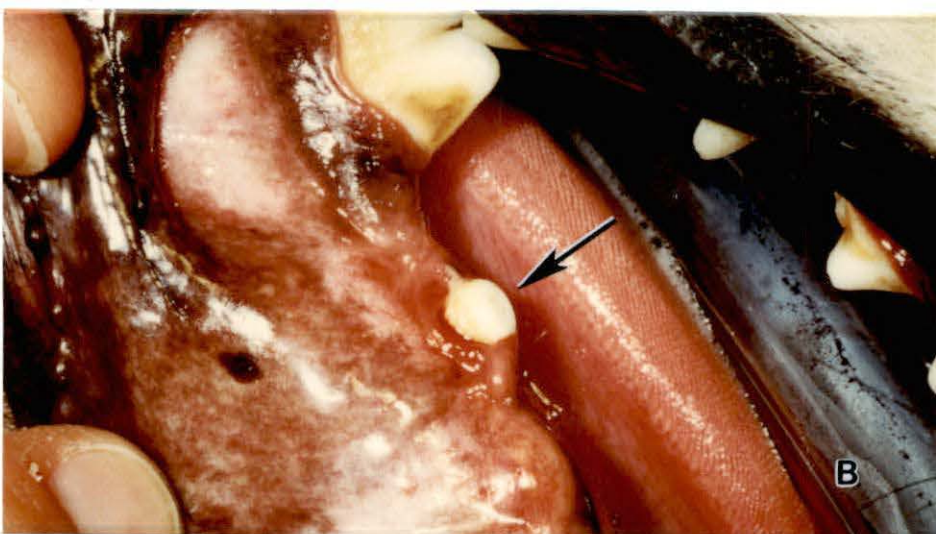
totally covered prior to the gingiva cut-back procedure. Some of the partial cut-throughs can be attributed to the same influences as listed for the 2 mm implants. The 4 mm implant cut through after 2 weeks and was also found to be too high at the time of implantation due to extreme stretching of the gingiva. Figure 20b shows the clinical response to the 4 mm implant after it had protruded through the gingiva. Figure 20c shows the clinical response at the 6 months evaluation period to irregular and smooth surfaced 2 mm implants.

All of the osteoceramic implants were retained during the entire evaluation periods. At the 9 months evaluation, two of the implants had broken off approximately midsection (Dogs 8725, 8734). Even though a large force was needed to fracture the ceramic, the bonding between the remaining tooth root and bone kept the bottom portion in place. One implant (8734) had a circumferential fracture of the ceramic above the groove, but the entire implant was still in place at 10 months. The radiographs in Figure 21 and 22 taken at 9 months show the bone response to the implants and the fractured implants.

The values for a particular index of each of the three implant surfaces were lumped together for each evaluation period. In doing this, the location of the implant, the

Figure 21.　Radiographs of osteoceramic implants, dog
8734 at 9 months after gingiva cut-back.　a)
right mandible, b) left mandible

A

B

Figure 22.   Radiographs of osteoceramic implants, dog 8725 at 9 months after gingiva cut-back. a) right mandible, b) left mandible
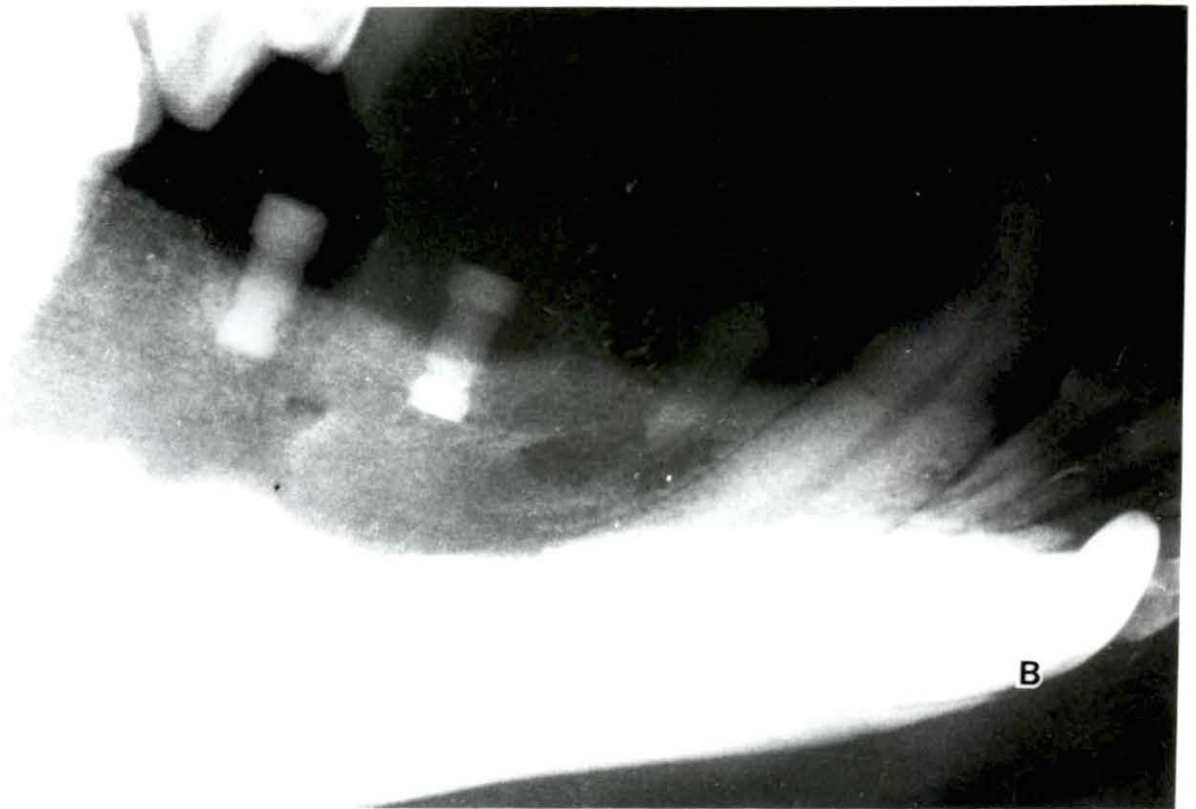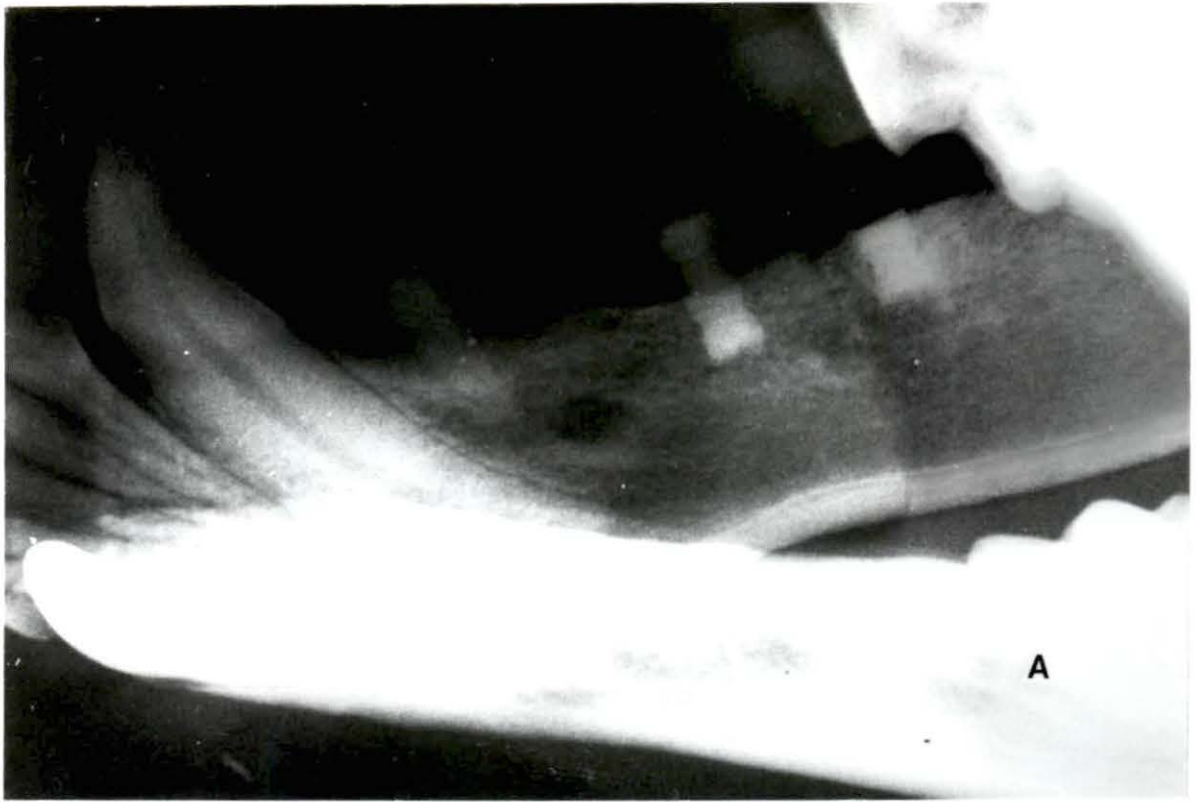
varying shoulder height and the host response of the dogs were assumed to have no significant effect. The location of the implants can be disregarded since the implant types had been randomly placed. There was variance of the index rating due to the subjective nature of this system.

To evaluate the index results, two comparisons were made. First, the results of the implants with the smooth and rough surfaces were compared with the irregular surface, which was the control surface. Second, the general osteoceramic response, which is the average of all surfaces of osteoceramic, was compared with the results found for the control teeth.

For the comparison between the smooth and rough surfaces and the control surface, if the means for a implant surface type at a specific evaluation period were more than two standards deviations (plus and minus) different from the mean of the control surface they were considered to be statistically different. The two standard deviations give a 95.5% confidence interval. Due to a low number of data points for several time periods, valid statistical comparison could not be made. Therefore, if the number of data points was less than 3, no comparison was made.

For the bleeding index results, no valid statistical difference between the smooth and rough surfaces and the control surface was found. All the surface types had a mobility index of 0, except for one rough implant type at the 2 week evaluation period. For this dog (8739), the buccal portion of the bone had receded to allow slight movement of the implant. No conclusion can be made whether this was due to the surface of the implant or other factors, such as implantation angle or patient response.

For the plaque and calculus index as well as the sulcus depth no valid statistical difference were found between the smooth and rough surface samples and the control samples.

Because the three surfaces showed no differences in their clinical response for the indexes used, all the osteoceramic results were averaged together for each index parameter and evaluation period and compared to the control teeth in Table 14. Table 18 gives the results for the general osteoceramic. For this analysis, standards given by Koth et al. (1985) and shown in Table 19 were used for comparison. Again, if the number of data points in the sample was smaller than 3, no comparison was made.

For the bleeding index results, the osteoceramic showed a higher value at 2 weeks and 4 months than the

Table 18. Clinical evaluation of the general osteoceramic implant

	Time Period							
	2 wks	1 mo	2 mo	3 mo	4 mo	5 mo	6 mo	9 mo
Bleeding Index	16[a] 2.40[b] (0.61)	8 1.66 (0.55)	8 2.60 (0.56)	14 1.11 (0.68)	10 2.69 (0.48)	6 2.36 (0.50)	8 2.60 (0.50)	6 2.67 (0.41)
Mobility Index	16 0.06 (0.25)	8 0	8 0	14 0	10 0	6 0	8 0	8 0
Plaque Index	16 1.47 (0.67)	8 1.5 (0.53)	8 1.52 (0.49)	14 1.57 (0.85)	10 1.78 (0.60)	6 2.17 (0.82)	8 2.75 (0.89)	6 2.92 (0.92)
Sulcus Depth (mm)	10 3.28 (1.21)	4 2.77 (1.31)	8 3.35 (1.36)	− − −	10 3.49 (0.94)	6 3.29 (0.87)	8 3.56 (0.83)	6 3.87 (0.60)
Radiograph Index	32 0.63 (0.71)	16 0.88 (0.81)	24 0.79 (0.78)	24 0.75 (0.74)	12 0.75 (0.75)	8 0.50 (0.53)	16 0.75 (0.68)	8 0.88 (0.83)
Ridge Loss (%)	32 -2.09 (4.18)	16 1.19 (8.53)	24 0.29 (6.54)	24 -1.75 (4.98)	12 0.08 (2.35)	8 -1.13 (3.00)	16 -1.44 (7.12)	8 -2.75 (6.14)

[a]Sample number.

[b]Mean (standard deviation).

Table 19. Acceptable standards for clinical success of
          endosteal implants (Koth et al., 1985)

Index	Accepted Index Standards
Gingival Bleeding	1.0 or less, or if 1.0 but < 2.0, no greater difference between implant and control than 0.5 units
Sulcus Depth	No minimum, but must not vary more than 3 mm between implant and control
Mobility	2.0 or less with cemented prosthesis, 1.0 or less if free standing
Plaque and calculus	No minimum, but must not vary more than 0.5 units between implant and control

control teeth. The higher value of the osteoceramic at 2
weeks is attributed to the recent cutting back of the
gingiva. At 4 months, the difference falls outside the
range of accepted standards. This result is not very
significant due to only 3 control samples, and because it
is not supported by a continued trend. The osteoceramic
mobility index was 0 for all evaluations periods except for
2 weeks where a value of 0.06 was found. Therefore, the
mobility index of the osteoceramic was acceptable.

For the plaque and calculus, a direct comparison at
each time period could not be made between the osteoceramic

and the control since the natural teeth were not cleaned
prior to the start of this experiment. The trend of the
osteoceramic implants was a steady increase in plaque. A
comparison made at 4 months showed a plaque and calculus
index of 1.78 ± 0.60 for the osteoceramic and 1.29 ± 0.51
for the control. The difference between these is within
the accepted standard. However, the acceptable standards
set by Koth et al. (1985) assume that plaque control must
be strongly enforced. For our research, no dental care was
given possibly making the plaque and calculus value much
higher.

For the sulcus depth measurements, no direct
comparison between the osteoceramic and the control could
be made due to the design of the shoulder. The
osteoceramic sulcus depth index was fairly constant with
the differences between the control teeth and the
osteoceramic being no larger than 1.84 mm.

Radiographic results

Radiographic evaluation included the radiographic
index and vertical alveolar ridge loss shown in Tables 14-
18. In these tables, a positive value for the ridge loss
denotes a gain in vertical height, whereas a negative value
denotes a loss. Radiographs of the implant/tissue blocks

were done to get both mesiodistal and buccolingual views. These radiographs taken of all the euthanized dogs are shown in Figures 23-30. The radiographs of the 12 months dogs taken at the 9 months evaluation period are shown in Figures 21 and 22.

For the 20 day and 33 day evaluation periods (8724, 8736), the radiographs showed good bone remodeling occurring around the implants. At 20 days, the average ridge loss was 2.13 ± 1.31% whereas at 33 days, the ridge had increased 4.13 ± 5.45%. This difference in response is most likely due to the variance in host response.

In positioning of the implants, the type of surface adjacent to the bone was always the irregular surface. The response of the bone should therefore be similar in all, unless the gingival attachment to the shoulder surfaces has a secondary effect on the underlying bone. Consequently, the radiographic index of the smooth and rough surfaces were compared to the control surface. As with the clinical results, if the mean for the radiographic index for an implant surface type at a specific evaluation period was no more than two standard deviations (plus and minus) different than the mean from the control, they were considered not to be statistically different. The radiographic index for the different surfaces showed no

Figure 23.   Radiographs of osteoceramic implants, dog
              8736 at 22 days after implantation. a)
              mesiodistal view, b) buccolingual view. R
              or L denotes right or left mandible. F or B
              denotes front or back position

Figure 24.   Radiographs of osteoceramic implants, dog
              8724 at 33 days after implantation. a)
              mesiodistal view, b) buccolingual view

Figure 25.   Radiographs of osteoceramic implants, dog
              8733 at 1 month after gingiva cut-back. a)
              mesiodistal view, b) buccolingual view

23

RF   RB   LF   LB   A

B

24

A

B

25

A

B
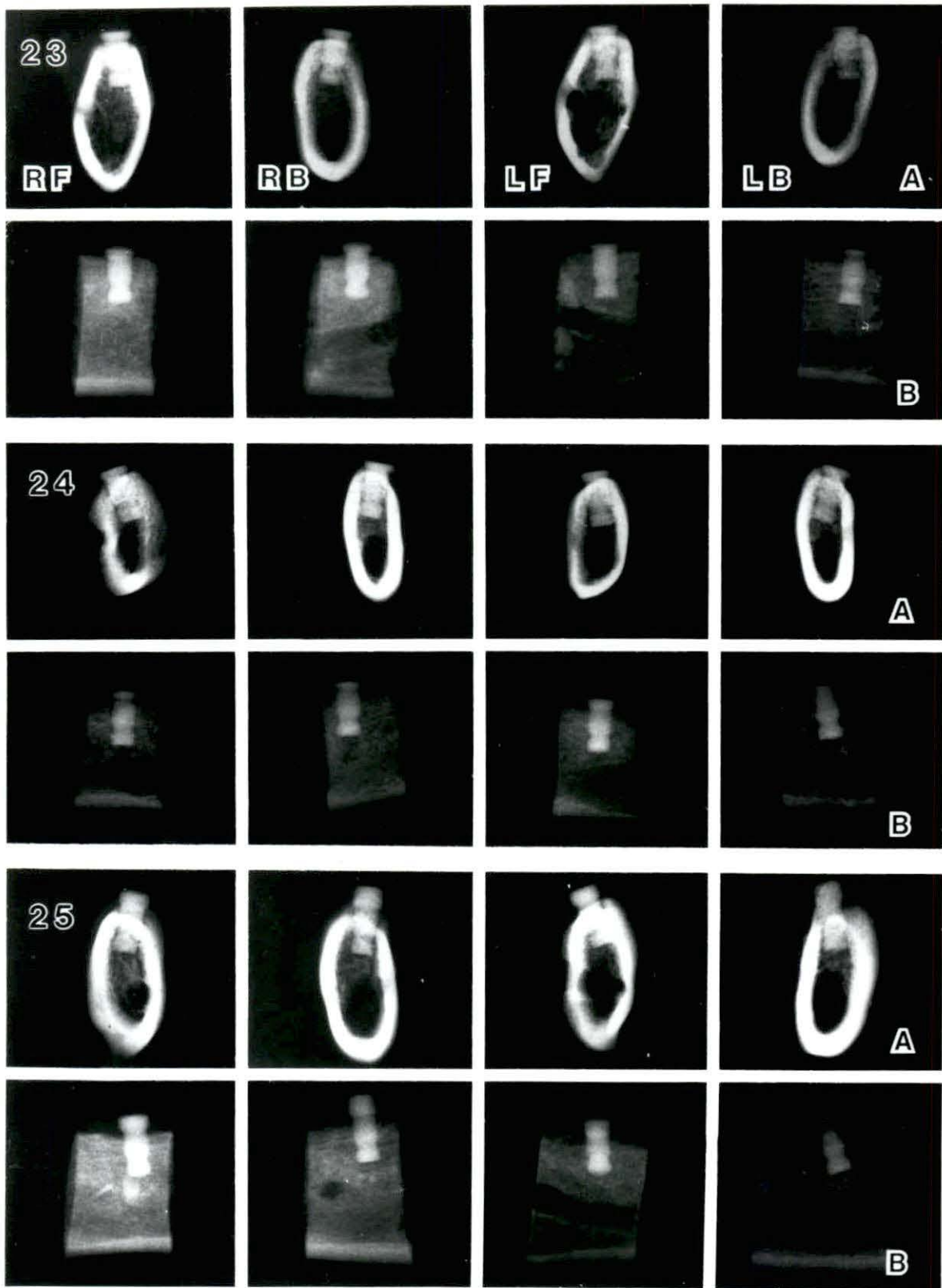
Figure 26.   Radiographs of osteoceramic implants, dog
              8739 at 1 month after gingiva cut-back. a)
              mesiodistal view, b) buccolingual view. R
              or L denotes right or left mandible. F or B
              denotes front or back position

Figure 27.   Radiographs of osteoceramic implants, dog
              7934 at 3 months after gingiva cut-back. a)
              mesiodistal view, b) buccolingual view

Figure 28.   Radiographs of osteoceramic implants, dog
              8730 at 3 months after gingiva cut-back. a)
              mesiodistal view, b) buccolingual view

26

RF RB LF LB A

B

27

A

B

28

A

B
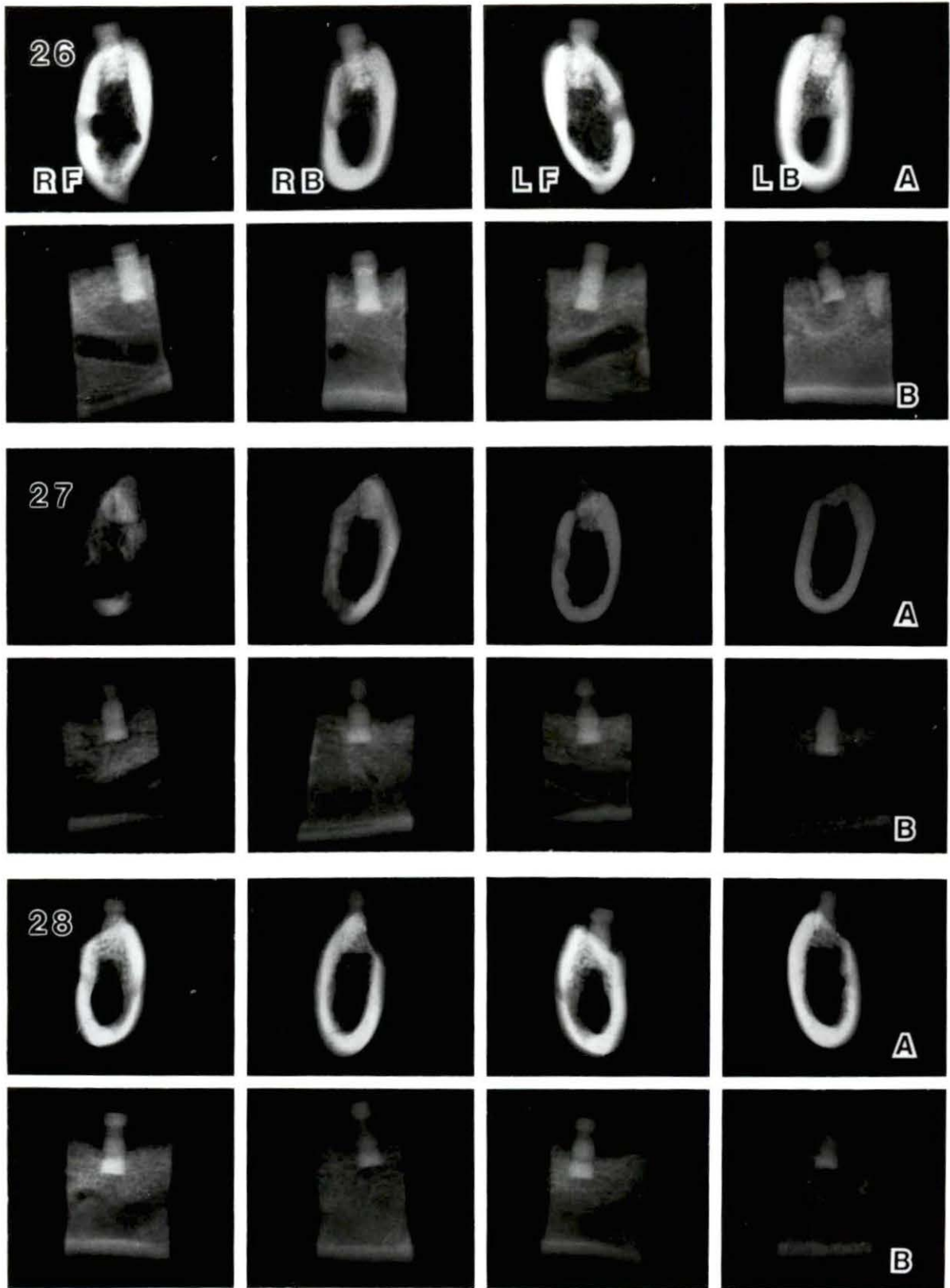
Figure 29.   Radiographs of osteoceramic implants, dog
              8722 at 6 months after gingiva cut-back. a)
              mesiodistal view, b) buccolingual view. R
              or L denotes right or left mandible. F or B
              denotes front or back position

Figure 30.   Radiographs of osteoceramic implants, dog
              8732 at 6 months after gingiva cut-back. a)
              mesiodistal view, b) buccolingual view

29

RF   RB   LF   LB   A

B

30

A

B
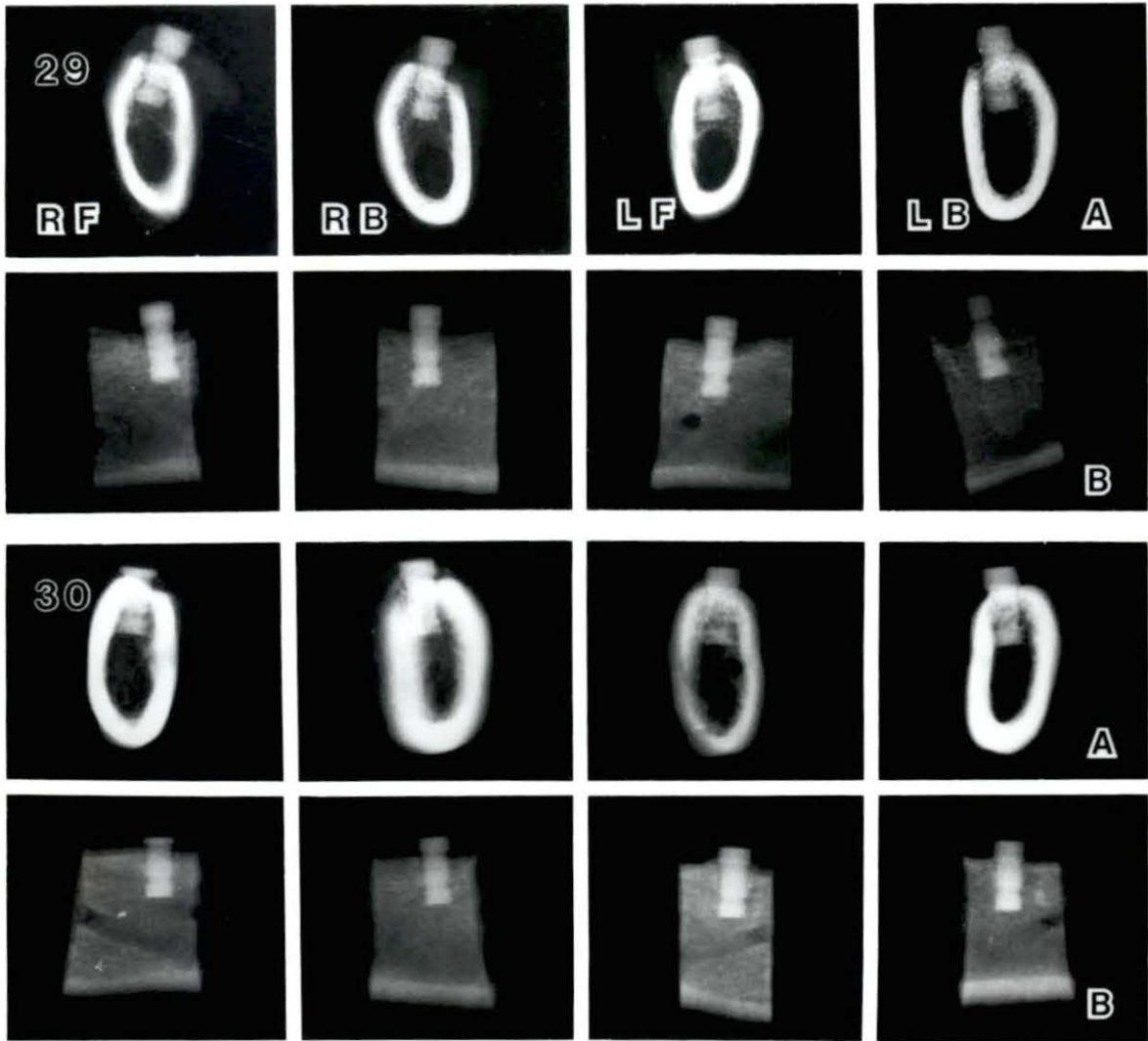
statistical differences from the control. The radiographic
index was also assessed on the radiographs prior to the
cut-back procedure to determine if exposure to the oral
environment affected the bone response. These results are
shown in Table 20. No difference in bone response between
the surfaces was found prior to cut-back. The mean for
osteoceramic radiographic index remained within the 0.5 and
0.88 for all evaluation periods showing that there was none
to slight resorption of the alveolar bone around the
implant.

Many dogs showed a general decrease in the alveolar
ridge height in the 2nd, 3rd, or 4th premolar regions. To
determine whether the surface variations had any effect,
the data from the smooth and rough surface samples were
compared with these from the control samples. For both the
pre cut-back data shown in Table 19 and the after cut-back
data, no difference in vertical alveolar ridge loss related
to surface variation was found. Further comparison was
made to determine if more ridge height was lost after the
gingiva had been cut back allowing exposure to the oral
environment. The ridge loss prior to cut-back for the
osteoceramic was 1.73 % while after the cutback it was 0.52
%. This concludes that the cut-back did not cause the
alveolar bone to recede more than prior to cut-back. The

Table 20. Radiographic evaluation of osteoceramic
surfaces prior to cut-back

		Time Period			
	Surface	2 weeks	4 weeks	6 weeks	8 weeks
Ridge Loss (%)	smooth	8[a] -4.63[b] (4.31)	8 0.13 (4.32)	1 -2.00 (-)	1 -2.00 (-)
	irregular	14 -5.36 (6.84)	14 0.43 (3.27)	9 0.22 (3.07)	5 0.80 (2.86)
	rough	10 -5.60 (5.82)	10 1.40 (3.06)	2 -1.00 (5.66)	2 -5.00 (8.50)
Radiographic Index	smooth	8 0.88 (0.35)	8 0.50 (0.76)	1 0 (-)	1 0 (-)
	irregular	14 0.79 (0.43)	14 0.50 (0.52)	9 0.56 (0.53)	5 0.80 (0.45)
	rough	10 0.60 (0.52)	10 0.40 (0.52)	2 0.50 (0.71)	2 0.50 (0.71)

[a]Sample number.

[b]Mean (standard deviation).

higher loss prior to cut back can be due to the vascular
disruption caused by the surgery.

Since the implants were not put in function, the alveolar bone loss can be due to lack of stimulation of the bone. This is supported by the fact that the ridge receded in the whole 2nd, 3rd, 4th, premolar region and not only adjacent to the implant. The classic failure response to dental implants shows resorption of bone surrounding the implants, but with most implants the bone maintained intimate contact with the implant as shown in the radiographic index results. A study done by Winter et al. (1974) found that the edentulous mandible in human loses an average of 1.6 mm of vertical alveolar bone height over a five year period. For our study the average bone loss at the 9 months evaluation period was 1.73 mm ± 0.74 mm, at 6 months 0.37 ± .75 mm, at 3 months 1.99 ± 3.07 mm, and at 1 month there was a 0.23 ± 0.74 mm gain in alveolar ridge. There is no linear trend in the loss with time, so the differences could be due to animal response.

Design Evaluation

The design of the implant worked well in controlling the depth of placement and in placing the different surfaces adjacent to the gingiva. The circumferential dimensions were adequate for all the dogs. From the buccolingual sections, the observation was made that a longer tooth root might have given the tooth root more

support by extending into the lower portion of the alveolar bone.

Even though all the implant edges had been smoothed, the edge of the shoulder especially must be rounded to keep it from cutting through the gingiva. The right angle between the shoulder and shaft may be disadvantageous to our design because bacteria and debris can deposit at that corner and cause infection. Further, it is uncertain how the biomechanical forces of the shoulder on the alveolar ridge affect its bone response. The forces may be beneficial in stimulating bone or detrimental in causing bone resorption, therefore future investigation should be done to examine this problem.

CONCLUSIONS

The manufacturing process to make three different surface structures produced a smooth surface with micropores, a slightly irregular surface with undulations, and a roughened surface with micro- and macropores.

The design of this implant was successful for the implantation method used for this project. Through the shoulder design, the three different surfaces were placed adjacent to the gingiva. With regard to shoulder height, the 2 mm shoulder was the most successful for this experimental procedure of keeping the implant covered during initial healing and then cutting the gingiva back to expose the shoulder of the implant. No statistically significant differences between the samples was found in the clinical and radiographic results. Future histological work to examine epithelial cells adjacent to the surface will give more information on the extent of attachment.

The osteoceramic was found to be clinically successful as an endosteal implant with regard to its mobility and radiographical indexes. The osteoceramic had more bleeding at earlier examinations than the control teeth which may be attributed to the cut-back procedure. Radiographically, the osteoceramic implant showed intimate bone contact existed and only slight resorption of the surrounding bone.

The vertical recession of the alveolar bone was attributed in part to the tooth roots not being in function. All of the implants were retained during the evaluation periods. At 9 months, two implants had broken off at midsection and one was cracked circumferentially.

Future recommendations in the development of this dental implant include making the tooth root functional by attaching a crown and to prestress the ceramic composite prior to implantation to increase its tensile strength. Also, the biomechanical forces produced by the implant shoulder in this design on the alveolar ridge should be examined.

APPENDIX

The following table lists the dates at which the experimental steps on each of the dogs were done. It also gives the implant types and their position in the mandibles.

	Dog Number									
Step	8732	8725	8722	8734	8730	7934	8739	8733	8736	8724
Extrac-tions	6-22[a]	5-18	6-27	5-17	5-17	6-20	5-19	5-18	6-22	6-26
Implants	10-6	10-2	10-25	11-6	11-15	2-6	2-8	2-15	5-3	5-18
R F[b]	1 IR	2 IR	3 IR	2 IR	3 IR	2 SM	2 RO	2 RO	1 IR	1 IR
R B	2 IR	4 IR	3 RO	2 SM	2 RO	3 IR	3 SM	3 SM	1 IR	1 IR
L F	2 IR	3 IR	3 SM	2 SM	2 RO	3 RO	3 IR	2 IR	1 IR	1 IR
L B	2.6 IR	2 IR	3 RO	2 RO	2 SM	3 SM	3 RO	3 RO	1 IR	1 IR
Checkups										
2 weeks	10-20	11-6	11-9	11-17	11-30	2-26	2-27	3-1	5-14	5-29
4 weeks	11-2	11-15	11-28	12-4	12-19	3-8	3-8	3-20		6-11
6 weeks	11-16	12-4	12-8							
8 weeks	12-1									
10 weeks										
Cut-back	12-1	12-4	12-8	12-4	1-29	3-8	3-8	3-20		
Checkups post cut-back										
2 week	12-19	12-19	12-20	12-19	2-15	3-20	3-22	3-29		
1 month					2-27	4-5				
2 months	1-25	1-25	1-30	1-30	3-27	5-4				
3 months	2-27	3-1	3-1	3-1						
4 months	4-12		4-10	4-5						
5 months	5-4		5-10							
6 months		6-4		6-4						
9 months		9-5		9-10						

Step	8732	8725	8722	8734	8730	7934	8739	8733	8736	8724
Dog Number										

Step	8732	8725	8722	8734	8730	7934	8739	8733	8736	8724
Bone labeling										
oxytetra[c]	5-5	11-9		11-5	3-28	5-7	3-30	4-4	5-5	5-20
demeclo[d]	4-12	9-5	4-12	9-5						6-11
xyl or[e]	5-4	10-8	5-8	10-11	4-13	5-18	3-22	3-29	5-14	5-29
aliz red[f]					4-20					
Euthan-asia	6-1	12-5	6-7	12-4	4-24	6-7	4-10	4-12	5-23	6-20
Total time after implantation in days									20	33
Total time after cutback in months	6	12	6	12	3	3	1	1		

[a]**6-22** = date in bold denoted 1989, all dates in normal format denote 1990.

[b]RF, RB, LF, LB = right (left) front (back) position of the implant in the mandible.

[c]Oxytetra = oxytetracycline.

[d]Demeclo = demeclocycline.

[e]Xyl or = xylenol orange.

[f]Aliz red = alizarin red S.

REFERENCES

Adell, R., U. Lekholm, B. Rockier, and P. I. Branemark. 1981. A 15-year study of osseointegrated implants in the treatment of the edentulous jaw. Int. J. Oral Surg. 10:387-416.

Atmaran, G. H., H. Mohammed, and F. J. Schoen. 1979a. Stress analysis of single-tooth implants, I. Effect of elastic parameters and geometry of implant. Biomater. Med. Devices Artif. Organs 7(1):99-104.

Atmaran, G. H., H. Mohammed, and F. J. Schoen. 1979b. Stress analysis of single-tooth implants, II. Effect of implant root-length variation and pseudo periodontal ligament incorporation. Biomater. Med. Devices Artif. Organs 7(1):105-110.

Baier, R. E., A. E. Meyer, J. R. Natiella, R. R. Natiella, and J. M. Carter. 1984. Surface properties determine bioadhesive outcomes: Methods and results. J. Biomed. Mater. Res. 18:337-355.

Balkin, B. E. 1988. Implant dentistry: Historical overview with current perspective. Pages 19-21 in NIH consensus development conference on dental implants, program and abstracts, June 13-15.

Banks, W. J. 1986. Applied Veterinary Histology. 2nd edition. Williams and Wilkins, Baltimore.

Boretos, J. W. 1985. Ceramics in clinical care. Am. Ceram. Soc. Bull. 64(8):1098-1100.

Branemark, P. I., U. Breine, R. Adell, B. O. Hansson, J. Lindestroem, and A. Ohlsson. 1969. Intra-osseous anchorage of dental prostheses. Scand. J. Plastic Reconstr. Surg. 3:81-100.

Bruneel, N. and J. A. Helsen. 1988. In-vitro simulation of biocompatibility of Ti-Al-V. J. Biomed. Mater. Res. 22:203-214.

Brunette, D. M., G. S. Kenner, and T. R. L. Gould. 1983. Grooved titanium surfaces orient growth and migration of cells from human gingival explants. J. Dent. Res. 62(10):1045-1048.

Brunski, J. B. 1988a. Biomechanics of oral implants:
     Future research directions. J. Dent. Educ. 52(12):775-
     787.

Brunski, J. B. 1988b. Implants: Biomaterials and
     biomechanics. CDA (California Dental Association) J.
     16(1):66-77.

Cameron, H. U., I. Macnab, and R. M. Pilliar. 1977.
     Evaluation of biodegradable ceramic. J. Biomed.
     Mater. Res. 11:179-186.

Campbell, C. E. and A. F. von Recum. 1989.
     Microtopography and soft tissue response. J.
     Investigative Surg. 2:51-74.

Colaizzi, F. A., N. S. Javid, C. G. Michael, and C. J.
     Gibbs. 1984. Biting force, EMG, and jaw movements in
     denture wearers. J. Dent. Res. 63:329.

Collins, P. J and C. A. Squier. 1980. Implant porosity -
     the effect on soft tissue attachment. J. Implant Dent.
     11:3-6.

Cook, S. D. and K. A. Thomas. 1990. Hydroxyapatite-coated
     metal for orthopedic and dental implant applications.
     A paper presented at the 92nd Annual American Ceramic
     Society Meeting, April 22-26, 1990, Dallas, Texas.

Coolidge, E. D. 1937. The thickness of the human
     periodontal membrane. J. Am. Dent. Assoc. 24:1260-1270.

Cranin, A. N., J. Gelbman, J. Dibling, and A. Simons.
     1988. The evaluation of the canine as a model for human
     dental implant research. A paper presented at the
     Symposium on Retrieval and Analysis of Surgical Implants
     and Biomaterials, Society for Biomaterials, Aug. 12.

Cutright, D., S. Bhaskar, M. Brady, L. Getter, and W.
     Posey. 1972. Reaction of bone to tricalcium phosphate
     ceramic pellets. Oral Surg. 33(5):850-856.

de Groot, K. 1980. Bioceramics consisting of calcium
     phosphate salts. Biomaterials 1:47-49.

de Groot, K. 1981. Pages 199-222 in D. F. Williams, ed.
     Biocompatibility of clinical implant materials. Vol. 1.
     CRC Press, Boca Raton, Florida.

de Groot, K. 1988. Effect of porosity and physiochemical properties on the stability, resorption, and strength of calcium phosphate ceramic. Annals of the New York Academy of Sciences 523:227-233.

de Groot, K., A. Tencer, P. Waite, J. Nichols, and J. Kay. 1988. Significance of the porosity and physical chemistry of calcium phosphate ceramics. Annals of the New York Academy of Sciences 523:272-277.

Denissen, H. W., H. J. A. van Dijk, A. P. Gehring, and K. de Groot. 1979. Preparation of densely sintered calciumhydroxyapatite. IADR 57th General Meeting, New Orleans, Abstract 613.

Denissen, H. W., K. de Groot, P. C. Makkes, A. Van den Hoof, and P. J. Klopper. 1980. Tissue response to dense apatite implants in rats. J. Biomed. Mater. Res. 14:713-721.

Eriksson, R. A. and T. Albrektsson. 1984. The effect of heat on bone regeneration: an experimental study in the rabbit using the bone growth chamber. J. Oral Maxillofac. Surg. 42:705-711.

Ehrnford, L., B. Sundstrom, and K. Wallenius. 1980. Bone tissue formation within a sintered microporous glass-fiber network implanted in extraction sockets in the rat. Scand. J. Dent. Res. 88(2):130-133.

Ferraro, J. W. 1979. Experimental evaluation of ceramic calcium phosphate as a substitute for bone grafts. Plastic and Reconstructive Surgery 63(5)634-640.

Freeman, J. W. 1972. Tissue response to varying surface finishes of titanium implants. South Carolina Dent. J. 30:10-13.

Gargiulo, A. W., F. M. Wentz, and B. Orban. 1961. Mitotic activity of human oral epithelium exposed to 30 percent hydrogen peroxide. Oral Surg. 14:474-492.

Graf, H. 1969. Bruxism. Dental Clinics North America 13:659-665.

Graves, A. M. 1988. Evaluation of a bioactive ceramic as an endosseous tooth root implant in sheep. M. S. Thesis. Parks Library, Iowa State University, Ames, IA.

Grenoble, D. E. and R. Voss. 1976. Materials and designs for implant dentistry. Biomater. Med. Devices Artif. Organs 4:133-169.

Hall, W. C., P. A. Cox, and S. R. McFarland. 1984. Some factors that influence prolonged interfacial continuity. J. Biomed. Mater. Res. 18:383-393.

Hannson, H.-A., T. Albrektsson, and P.-I. Branemark. 1983. Structural aspects of the interface between tissue and titanium implants. J. Prosthet. Dent. 50(1):108-113.

Harris, W. H., D. F. Travis, U. Friberg and E. Radin. 1964. The *in-vivo* inhibition fo bone formation be alizirin red S. The Journal of Bone and Joint Surgery 46A(3):493-508.

Hassler, C. R., R. H. Downes, L .G. McCoy, and L. C. Clark. 1983. Bone-ceramic interface of endosseous alumina implants. Pages 666-677 in L. R. Rubin, ed. Biomaterials in reconstructive surgery. C. V. Mosby, St. Louis.

Heimke, G. 1987. Ceramics for osseo-integrated implants. Advanced Ceramic Materials 2(4):764-770.

Heimke, G., B. D'Hoedt, and W. Schults. 1987. Ceramics in dental implantology. Pages 93-104 in A. Pizzoferrato, P. G. Marchette, A. Ravaglioli, and A. J. C. Lee, ed. Biomaterials and Clinical Applications. Elsevier Science Publishers, B. V., Amsterdam.

Heughebaert, J. C. and G. Bonel. 1986. Composition, structures, and properties of calcium phosphates of biological interest. Pages 9-14 in P. Christel, ed. Biological and Biomechanical Performance of Biomaterials. Elsevier Scientific Publishing Company, New York.

Hulbert, S. F., J. C. Bokros, L. L. Hench, J. Wilson, and G. Heimke. 1987. Ceramics in clinical applications, past, present, and future. Pages 3-27 in P. Vinvenzini, ed. High tech ceramics. Elsevier Science Publishers, B. V., Amsterdam.

Janikowski, T. and T. D. McGee. 1969. Artificial teeth for permanent implantation. Proc. Iowa Acad. Sci. 76:113-118.

Jarcho, M.   1986.   Biomaterial aspects of calcium
    phosphates: Properties and applications.
    Reconstructive Implant Surgery and Implant
    Prosthodontics.   Dental Clinics of North America
    30(1):25-47.

Jarcho, M., C. H. Bolen, M. B. Thomas, J. Bobick, J. F.
    Kay, and R. H. Doremus.   1976.   Hydroxylapatite
    synthesis and characterization in dense polycrystalline
    form.   J. Mater. Sci. 11:2027-2035.

Jarcho, M., R. L. Salsbury, M. B. Thomas, and R. H.
    Doremus.   1979.   Preparation and thermal properties of
    dense polycrystalline oxyhydroxyapatite.   J. Am. Ceram.
    Soc. 62:455-460.

Junqueria, L. C. and J. Carneiro.   1980.   Basic Histology.
    3rd ed.   Lange Medical Publications, Los Altos,
    California.

Karagianes, M. T., R. E. Westerman, J. J. Rasmussen and R.
    P. Marshall.   1974.   Development and evaluation of
    porous ceramic and titanium alloy dental anchors
    implanted in miniature swine.   J. Biomed. Mater. Res.
    Symposium 5(2)391-399.

Karagianes, M. T., R. E. Westerman, J. J. Rasmussen and A.
    M. Lodel.   1976.   Development and evaluation of porous
    dental implants in miniature swine.   J. Dent. Res.
    55:85-93.

Kent, J. N., M. S. Block, I. M. Finger, L. Guerra, H.
    Larsen, and D. J. Misiek.   1990.   Biointegrated
    hydroxylapatite-coated dental implants: 5-year
    clinical observations.   J. Am. Dent. Assoc. 121:138-144.

Klawitter, J. J., M. Weinstein, L. J. Peterson, R.
    Topazin, and R. V. McKinney, Jr.   1975.   A study to
    determine the histological acceptance of artificial
    teeth fabricated from different materials compositions.
    Submitted to Dept. of Health, Educ. and Welfare, Nat.
    Inst. for Dental Research #NO1-DE-32420, May 31.

Klein, C. P. A. T., A. A. Driessen, and K. de Groot.   1984.
    Relationship between the degradation behavior of calcium
    phosphate ceramics and their physical-chemical
    characteristics and ultrastructure geometry.
    Biomaterials 4(3):157-160.

Koth, D. L., R.V. McKinney, Jr., and D. E. Steflik. 1985. A clinical evaluation of the implant-gingival tissue interface. Pages 114-130 in R.V. McKinney and J. E. Lemons, eds. The dental implant: Clinical and biological applications. PGS, Littleton, Massachusetts.

Kronfeld, R. 1931. Histologic study of the influence of function of the human periodontal membrane. J. Am. Dent. Assoc. 18:1242-1274.

Lazzari, E. P. 1976. Dental Biochemistry. 2nd ed. Lea and Febiger, Philadelphia.

Lefevre, M. L. and H. G. Hodge. 1937. Chemical analysis of tooth samples composed of enamel, dentine and cementum. J. Dent. Res.16:279-287.

LeGeros, R. Z., J. R. Parsons, G. Daculsi, F. Driessens, D. Lee, S. T. Liu, S. Metsger, D. Peterson, and M. Walker. 1988. Significance of the porosity and physical chemistry of calcium phosphate ceramics: Biodegradation-bioresorption. Annals of the New York Academy of Sciences 523:268-271

Lemons, J. E. 1983. Phase-boundary interactions for surgical implants. Pages 662-665 in L. R. Rubin, ed. Biomaterials in reconstructive surgery. C. V. Mosby, St. Louis.

Lemons, J. E., N. Z. Ramsey, and E. K. Chamoun. 1988. Dental implant device retrieval. A paper presented at the Symposium on Retrieval and Analysis of Surgical Implants and Biomaterials, Snowbird, Utah, Aug.

Listgarten, M. A. 1966. Electron microscopic study of the dentogingival junction of man. Am. J. Anat. 119:147-155.

Loe, H. 1967. The structure and physiology of the dento-gingival junction. Pages 415-455 in A. W. Miles, ed. Structural and chemical organization of teeth. Vol 2. Academic Press, New York.

Marks, Jr., S. C. and S. N. Popoff. 1988. Bone cell biology: The regulation of development, structure and function of the skeleton. Am. J. Anat. 183:1-44.

Matlaga, F. B., L. P. Yasenchak, and T. N. Salthouse. 1976. The significance of implant shape in experimental testing of biological materials: Disc vs. rod. J. Biomed. Mater. Res. 10:391-397.

McDavid, P. T., M. E. Boone, A. H. Kafrawy, and D. F. Mitchell. 1979. Effect of autogenuous marrow and calcitonin on reactions to a ceramic. J. Dent. Res. 58(5):1478-1483.

McGee, T. D. 1974. United States Patent 3,787,900.

McGee, T. D. and J. L. Wood. 1974. Calcium-phosphate magnesium-aluminate osteoceramics. J. Biomed. Mater. Res. Symposium 5(1)137-144.

McKinney, Jr., R. V., D. L. Koth and D. E. Steflik. 1982. The single crystal sapphire endosseous dental implant. II. Two year results of clinical animal trials. J. Oral Implantology 10:619-638.

McKinney, Jr., R. V., D. E. Steflik and D. L. Koth. 1984. The biologic response to the single crystal sapphire endosteal dental implant: Scanning electron microscopic observations. J. Prosthet. Dent. 51(3)372-379.

McKinney, Jr., R. V., D. E. Steflik and D. L. Koth. 1985. Evidence for junctional epithelial attachment to ceramic dental implants: A transmission electron microscopy study. J. Periodontology 56:579-591.

Melcher, A. H. 1969. Healing of Wounds. Pages 429-529 in A.H. Melcher and W.H. Bowen, ed. Biology of the periodontium. Academic Press, New York.

Melcher, A. H. and J. E. Eastone. 1969. The connective tissues of the periodontium. Pages 167-343 in A.H. Melcher and W. H. Bowen, ed. Biology of the periodontium. Academic Press, New York.

Naray-Szabo, Istvan. 1969. Inorganic crystal chemistry. Akademiai Kiado, Budapest.

Natiella, J. R. 1986. Odontocompatibility assessment. Pages 339-348 in A. von Recum, ed. Handbook of Biomaterials. Macmillan Pub. Co., New York.

Niznick, G. A. 1985. Implant prosthodontics, a team approach. J. Oral Implantology 12(1):1-24.

Park, J. B. 1987. Biomaterials Science and Engineering. 2nd ed. Plenum Press, New York.

Ranly, D. M. 1976. Bone apposition and resorption. Pages 134-161 in E. P. Lazzari, ed. Dental biochemistry. 2nd ed. Lea and Febiger, Philadelphia.

Richardson, Jr., W. C., J. J. Klawitter, B. W. Sauer, J. R. Pruitt, and S. F. Hulbert. 1975. Soft tissue response to four dense ceramic materials and two clinically used biomaterials. J. Biomed. Mater. Res. Symposium 6:73-80.

Salthouse, T. N. 1984. Some aspects of macrophage behavior at the implant interface. J. Biomed. Mater. Res. 18:395-401.

Salthouse, T. N. and B. F. Matlaga. 1975. An approach to the numerical quantification of acute tissue response to biomaterials. Biomater. Med. Devices Artif. Organs 3:47-56.

Salthouse, T. N. and B. F. Matlaga. 1983. Some cellular effects related to implant shape and surface. Pages 40-45 in L. R. Rubin, ed. Biomaterials in reconstructive surgery. C. V. Mosby, St. Louis.

Schnitman, P. A. and L. B. Shulman, eds. 1980. Dental Implants: Benefit and Risk. An NIH-Harvard Consensus Development Conference. Bethesda, Maryland, United States Department of Health and Human Services. Publication No. (NIH) 81-1531.

Smith, C. J. 1969. Gingival Epithelium. Pages 105-166 in A. H. Melcher and W. H. Bowen, eds. Biology of the periodontium. Academic Press, New York.

Spence, A. P. and E. B. Mason. 1987. Human Anatomy and Physiology. 3rd ed. Benjamin/Cummings Publishing Co., Reading, Massachusetts.

Squier, C. A., A. W. Romanowski, and P. Collins. 1988. Soft tissue attachment at an implanted surface. Pages 121-126 in R. Skalak and C. F. Fox, eds. Tissue Engineering. Proceedings of workshop held Feb. 26-29. Alan R. Liss, Inc., New York.

Stanley, H. R., A. E. Clark, M. B. Hale, C. King, F. Colaizzi, D. Spilman and L. L. Hench. 1986. Clinical trials of bioglass implants for alveolar ridge maintenance. Trans. Soc. Biomat. 9:150.

Tweden, K. S. 1987. A comparison of four endosseous dental implants: Single-crystal sapphire; pyrolytic carbon; an alloy of titanium, aluminum, and vanadium; and a biologically active ceramic. Ph. D. Dissertation. Parks Library, Iowa State University, Ames, IA.

van Blitterswijk, C. A., J. J. Grote, W. Kuijpers, C. J. G. Blok van Hoek, and W. Th. Daems. 1985. Bioreactions at the tissue/hydroxyapatite interface. Biomaterials 6:243-251.

Vogel, J. J. 1976. Mineralization of Bones and Teeth. Pages 99-111 in E. P. Lazzari, ed. Dental biochemistry. 2nd ed. Lea and Febiger, Philadelphia.

Winter, C. M., J. B. Woelfel, and T. Agarashi. 1974. Five-year changes in the edentulous mandible as determined on oblique cephalometric radiographs. J. Dent. Res. 53(6):1455-1467.

Williams, D. F. 1981. Biocompatibility of clinical implant materials. Vol. 1. CRC Press, Inc., Boca Raton, Florida.

Worthington, P. 1988. Current implant use. Pages 27-30 in NIH consensus development conference on dental implants, Program and Abstracts, June 13-15.

ACKNOWLEDGEMENTS

I wish to thank my major professor, Dr. Thomas McGee, for his guidance and enthusiasm for this research project. My appreciation goes to the remaining committee members, Dr. Mary Helen Greer, Dr. Joseph Haynes, and Dr. William Hoefle for their advice and willingness to serve on the committee. Special thanks go to Dr. Ray Kudej for his suggestions and surgical expertise, which were invaluable. My appreciation is also extended to Bruce Wagner for his interest and help with the scanning electron microscopy and image analysis work. I want to thank all my friends, colleagues, and staff for their suggestions and assistance.

This work is dedicated to the special people in my life: to my husband Mark, for his unending encouragement and love; and especially to my parents Hannelore and Walter Gruss, for their continuous guidance and support, and for giving me the opportunities in life to make all this possible.

Lederle Laboratories are acknowledged for their donation of the demeclocycline bone labeling substance used in this research.